Determining the Differences in Effect of Chromate, Chromite and Chromium Picolinate in Rainbow Trout (*Oncorhynchus mykiss*) at Environmentally Relevant Concentrations

by

Chase R. Tudor

A thesis submitted to the
School of Graduate and Postdoctoral Studies in partial
fulfillment of the requirements for the degree of

Master of Science in Applied Bioscience

The Faculty of Science

University of Ontario Institute of Technology (Ontario Tech University)

Oshawa, Ontario, Canada

November 2021

THESIS EXAMINATION INFORMATION

Submitted by: **Chase Tudor**

Master of Science (MSc) in Applied Bioscience

Thesis title: Determining the Differences in Effect of Chromate, Chromite and Chromium Picolinate in Rainbow Trout (Oncorhynchus mykiss) at Environmentally Relevant Concentrations

An oral defense of this thesis took place on December 3rd, 2021, in front of the following examining committee:

Examining Committee:

Chair of Examining Committee	Dr. Janice Strap
Research Supervisor	Dr. Denina Simmons
Examining Committee Member	Dr. Julia Green-Johnson
Examining Committee Member	Dr. Gretchen Lescord
Thesis Examiner	Dr. Hélène LeBlanc

The above committee determined that the thesis is acceptable in form and content and that a satisfactory knowledge of the field covered by the thesis was demonstrated by the candidate during an oral examination. A signed copy of the Certificate of Approval is available from the School of Graduate and Postdoctoral Studies.

ABSTRACT

The Ring of Fire is a region in the James Bay Lowlands of northern Ontario that houses a rich deposit of chromite and is slated for mining development. The goals of this study were to better understand the relative effects of Cr^{6+} to Cr^{3+} in rainbow trout, identify potential protein biomarkers to distinguish between Cr^{6+} and Cr^{3+} exposure, and determine whether chromium picolinate (a commonly prescribed nutritional supplement) is beneficial or harmful to fish. Proteomic analysis on the fish plasma showed no difference in Cr^{6+} and Cr^{3+} exposure across all concentrations and between chromium species. Decreased abundance in proteins associated with hepatocellular carcinoma and cardiomyopathy were also observed. These proteins were Trim21, Slc8a1, Myh4 and Myh6. For all, decreased abundance is associated with adverse outcomes. We hope that this study will advance knowledge on chromium toxicity in fish and protect all that inhabit the Ring of Fire region of Canada.

Keywords: Chromium; Metals; Proteomics; Toxicology; Ring of Fire

AUTHOR'S DECLARATION

I hereby declare that this thesis consists of original work of which I have authored. This is a true copy of the thesis, including any required final revisions, as accepted by my examiners.

I authorize the University of Ontario Institute of Technology (Ontario Tech University) to lend this thesis to other institutions or individuals for the purpose of scholarly research. I further authorize University of Ontario Institute of Technology (Ontario Tech University) to reproduce this thesis by photocopying or by other means, in total or in part, at the request of other institutions or individuals for the purpose of scholarly research. I understand that my thesis will be made electronically available to the public.

The research work in this thesis that was performed in compliance with the regulations of Research Ethics Board/Animal Care Committee under **REB Certificate number/Animal care certificate file number 15916**.

_____ Chase Tudor

STATEMENT OF CONTRIBUTIONS

The total chromium and speciation analysis described in Chapter 2 was performed by Dr. Gretchen Lescord and her team at Laurentian University. I was only responsible for sample collection and preservation before sending them to her lab for analysis.

I hereby certify that I am the sole author of this thesis and that no part of this thesis has been published or submitted for publication. I have used standard referencing practices to acknowledge ideas, research techniques, or other materials that belong to others. Furthermore, I hereby certify that I am the sole source of the creative works and/or inventive knowledge described in this thesis.

ACKNOWLEDGEMENTS

This research project was conducted during the COVID-19 pandemic. Our university was shut down during the Summer of 2020, which is when the majority of my work should have been completed. As a result, all of my exposures and sample collection had to be completed during the fall semester while I was also a TA for four undergraduate biology courses, prepping for my seminar that was pushed from April to September and taking a mandatory GIS & Spatial Analysis course. Furthermore, delays in the supply chain caused some portions of this study to be changed completely at the last minute because, items required to perform our desired assays could not be procured in time.

A huge thank you to Dr. Linda Lara-Jacobo for putting together a protocol and collecting that material for me to conduct the micronucleus assay when my plans for a different assay fell through at the less than a week before I was supposed to start my exposures. This study come together because of her constant willingness to help and share her knowledge.

Thanks to all of the members of the Aquatic Omics Lab (Shreya Jain, Linda Jacobo, Urvi Pajankar, Meera Sidhu, Eric Porche, Fatima Bah, David McNabney, Simon Pollard, Nancy Tanouri and Tina Flaherty) who helped me collet my samples.

Thank you to my supervisor Dr. Denina Simmons. My journey into this master's degree was not a conventional one, and without her belief in me, none of this would have been possible.

Thank you to my family for supporting me on this journey. Their guidance and encouragement always push me to achieve more.

Finally, a special thank you to my loving partner Camille Carolissen. My gratitude for her is immeasurable. She was my guiding light to the very end. Without her support, and optimism throughout this process, I would have never finished.

TABLE OF CONTENTS

LIST OF TABLES

CHAPTER 2

CHAPTER 3

LIST OF FIGURES

CHAPTER 1

CHAPTER 2

CHAPTER 3

LIST OF ABBREVIATIONS AND SYMBOLS

ANOVA	Analysis of Variance
BGC	Blood Glucose Concentration
BN	Binucleated (same as split nuclei)
CPDB	Consensus Path Database - Human
DI	Deionized Water (Produced by reverse osmosis)
DMSO	Dimethylsulfoxide
DNA	Deoxyribonucleic Acid
GO	Gene Ontology
HDPE	High Density Polyethylene
HOGS	Human Ortholog Gene Symbols
HPA	Human Protein Atlas
HSD	Honest Significant Difference
HSI	Hepatosomatic Index
$ICDA_{CR}$	International Chromium Development Association
LC_{50}	Lethal Concentration expected to kill 50% test animals
LC-MS/MS	Liquid chromatography-tandem mass spectrometry
MDL	Minimum Detection Limit
MPP	Mass Profiler Professional
NT	Notched Nuclei
ppb	Parts Per Billion (1 µg/L = 1 µg/L = 1 ng/mL)
Q-TOF	Quadrupole Time of Flight
RBC	Red Blood Cell

Chapter 1. Introduction

1.1 Ring of Fire, Ontario, Canada

The Ring of Fire is a region in the James Bay Lowlands of northern Ontario, slated for mining development (1). The 2127 km^2 region houses several highly desired resources such as nickel, copper and gold, but most importantly, it is home to the world's richest deposit of chromite (1). It is also a part of the world's largest peatland, as well as a part of the traditional territory of several Indigenous communities (1). Of the 24.5 million tonnes of chromite that was produced internationally in 2012, only 31250 tonnes were produced in North America (1). According to a report conducted by the Ontario Chamber of Commerce (OCC) in 2014, there is an estimated 220 million tonnes of chromite contained within the Ring of Fire region. This deposit has been publicly valued by the government at between $30 – 60 billion. If development continue forward as planned, the Ring of Fire mining operation will be a highly valued asset in the Ontario and Canadian economy.

1.2 Overview of Chromium

Chromium exists in seven oxidation states, ranging from 0 to +6 (2). The most stable states, and therefore, the most common in the environment are +3 (Trivalent), +6 (Hexavalent) and +2 (2). Chromium is a very common metal used in industry for paints and dyes, leather tanning, metal plating, nutritional supplementation, and most notably, making non-corrosive alloys. Approximately 70% of the world's chrome is used for stainless steel production (ICDACR, 2020). Chromium in the form of ferrochrome, is one of the main components of stainless steel (1). This requires the smelting of chromite ore (1). The smelting process can result in the formation of Cr^{6+} as a by-product. Due to the geography of the Ring of Fire region, Cr^{6+} and Cr^{3+} contamination in the water is a possibility (1).

1.3 General Chromium Toxicity

The reported levels of toxicity for Cr^{3+} and Cr^{6+} vary within the literature. Some papers will report no or negligible adverse outcomes from ingestion, while others will find a number of detrimental toxic and carcinogenic effects (3-10). Cr^{6+} is considered a human lung carcinogen when inhaled, while Cr^{3+} is often considered an essential nutrient (4, 7, 11). However, the toxicity of Cr^{6+} is less certain when it comes to ingestion (4, 7). This is because Cr^{6+} is readily reduced to Cr^{3+} in acidic environments, such as the stomach (12). In addition, since Cr^{3+} is considered essential, the significance of Cr^{6+} ingestion seems to get overlooked, due to conversion early in the digestion process (12). This is an important concern when it comes to subsistence communities that depend on wild fish that could become contaminated with Cr^{6+} in the Ring of Fire region (13). Moreover, Cr^{3+} has its own genotoxic effects, due to its involvement with the formation of genotoxic adducts (14). Even though this information is readily available within the literature, Cr^{3+} in the form of chromium picolinate is marketed and sold as a weight loss/anti-diabetic nutritional supplement. Furthermore, there is also a lot of inconsistency within the literature as to whether or not Cr^{3+} is an essential nutrient (3, 10, 11, 15, 16). This aspect of chromium will not be explored by this study; however, it emphasizes the point that chromium is understudied and the state of opinion on chromium toxicity within the literature is indeterminate. Chromium in its hexavalent form can result in carcinogenic, genotoxic, cytotoxic and neurotoxic effects (1, 17, 18). Cr^{3+} has been shown to be genotoxic due to its role in DNA adduct formation (14, 17, 19). Water contamination with either of these chromium species could result in potential negative impacts on local wildlife, as well as Indigenous communities whom rely on wild fish as a staple in their diets (20).

1.4 Chromium Toxicity in Fish

Research on the exposure of fish to chromium has gleaned a number of different negative impacts on processes such as survival, development and metabolism. Tilapia exposed to Cr^{6+} concentrations ranging from 10 mg/L to 30 mg/L resulted in substantial chromium accumulation in organs and tissues that ranged from 0.86 – 45.23 µg/g (21). This was also the case at concentrations below the drinking water maximum acceptable concentration (MAC) of 50 µg/L (21). These effects can even impact fish reproduction (22). Chronic Cr^{6+} exposure was shown to decrease egg weight and fertilization rates in Japanese medaka (*Oryzias latipes*) by approximately 20% (22). Prolonged exposure to Cr^{6+} alters the overall survival rates of the fish (21). Furthermore, the pH of the environment also plays a significant role in Cr^{6+} toxicity, and even has an additive effect on the negative impact on fish mortality (23). This was shown to be most pronounced with regards to Cr^{6+} accumulation in the gill, with greater tissue concentrations at pH 6.5, than 7.8 (23). From a development/growth perspective, Cr^{6+} exposure will also result in negative outcomes. Japanese medaka (*Oryzias latipes*) exposed to Cr^{6+}, exhibit decreased liver, gill, and intestine weights, while the hepatosomatic index (HSI) remained the same (24). HSI is a measure of the energy reserves in an animal, especially in fish. An unchanged HSI, even though the liver mass is reduced, indicates that the overall somatic proportions of the fish have decreased. Moreover, these reductions in mass may be attributed to a decrease in feeding behaviour. A Cr^{6+} exposure study conducted on rainbow trout (*Oncorhynchus mykiss*) at 10 mg/L, resulted in an 8% reduction in initial mass when compared to the control group, which gained approximately 6% (25). It was concluded that a decrease in displayed feeding behaviour was responsible for the 14% difference in mass (25). Lastly, Cr^{6+} can also have a significant negative effect on fish metabolism. This has been shown in a number of studies where a decrease in muscle and liver glycogen stores (26, 27). These decreased glycogen levels are observed after prolonged exposure to Cr^{6+} (26, 27). Cr^{6+}

causes a number of problems in a variety of body systems making it vital to understand how this metal behaves within organisms.

1.5 Chromium Reduction

Higher oxidation states of chromium are reduced within the body by stomach acid. However, if some of that chromium is not fully reduced, or takes a different route of exposure such as inhalation, there may still be other reductive mechanisms involving endogenous reducing agents. Major reducers of hexavalent chromium within cells are ascorbic acid (vitamin C), cysteine, and glutathione (17). It has been shown in an *in vitro* study, using *E. coli* plasmid pBR322 DNA and calf thymus DNA, that when Cr^{6+} is reduced by ascorbic acid, the reaction intermediates Cr^{4+} and Cr^{5+}, are able to produce Cr – DNA adducts and single-strand DNA breaks (14, 28). In neutral aqueous solutions, Cr^{6+} reduced by cysteine produces small amounts of the relatively stable thiol complex, N(cis),O(cis),S(trans)-bis(L-cysteinato(2-))chromate(III) (29). Glutathione reduces Cr^{6+} by acting as a monodentate ligand and will bind at the cysteinyl thiolate group, forming a chromium-glutathione adduct (19, 30). All reductions will result in the eventual formation of a Cr^{3+} molecule and/or the aforementioned intermediates and by-products (19, 29).

A three-step mechanism is the most common process for Cr^{6+} reduction with one electron donor (31, 32). Simply put, Cr^{6+} will keep gaining electrons until it is in a stable Cr^{3+} form (31, 32). Both Cr^{4+} and Cr^{5+} molecules are produced as intermediates during the reaction but are short lived because of their poor stability (31, 32). The reactions occur as follows, where "D" is the electron donor:

$$Cr^{6+} + D^{n+} \longrightarrow Cr^{5+} + D^{(n+1)+} \quad \textbf{[1]}$$

$$Cr^{5+} + D^{n+} \longrightarrow Cr^{4+} + D^{(n+1)+} \quad \textbf{[2]}$$

$$Cr^{4+} + D^{n+} \longrightarrow Cr^{3+} + D^{(n+1)+} \quad \textbf{[3]}$$

More complex reactions can also take place with different substrates that can be one or two electron donors (31, 32). In these mechanisms, a Cr^{6+}-substrate complex is formed, followed by either a one, or two electron transfers (31, 32). A single electron transfer will result in the formation of Cr^{5+} a free radical, while the transfer of two electrons will yield Cr^{6+} and a product that will vary depending on what the starting substrate was (31-33):

$$Cr^{6+} + S \rightleftharpoons Cr^{6+} - S \quad \textbf{[4]}$$

$$Cr^{6+} - S \longrightarrow Cr^{4+} + P \quad \textbf{[5]}$$

$$Cr^{6+} - S \longrightarrow Cr^{5+} + R^{*} \quad \textbf{[6]}$$

Many other mechanisms are possible due to the high reactivity of Cr^{6+} intermediates (31, 32). Common cellular reductants for Cr^{6+} are thiols such as glutathione and cysteine as well as reduction by ascorbate (34). Thiol reduction initiates with the formation of a Cr^{6+} thioester that reacts with another thiol molecule, resulting in a Cr^{4+} intermediate and an oxidised disulfide product (31, 35, 36). Secondarily, the Cr^{4+} molecule could go through an intermolecular redox reaction, resulting in Cr^{5+} and a thiyl radical (31, 35, 36). The general mechanism where "RSH" represents the thiol, is depicted below:

$$Cr^{6+} + RSH \rightleftharpoons Cr^{6+}SR \quad \textbf{[7]}$$

$$Cr^{6+}SR + RSH \longrightarrow Cr^{4+} + RSSR \quad \textbf{[8]}$$

$$Cr^{6+}SR \longrightarrow Cr^{5+} + RS^{*} \quad \textbf{[9]}$$

Ascorbate reduction is initiated by Cr^{6+} and an ascorbate anion reacting to form a Cr^{6+} - ascorbate adduct (31, 37). The adduct then dissociates, producing Cr^{4+} and an ascorbate derived carbon molecule (31, 37). Lastly, Cr^{4+} will react with another ascorbate molecule and produce Cr^{3+} and an ascorbate free radical (31, 37). The mechanism for this is as follows below, where "RH^-" represents ascorbate (31):

$$Cr^{6+} + RH^- \rightleftharpoons Cr^{6+}RH \quad \textbf{[10]}$$

$$Cr^{6+}RH \rightleftharpoons Cr^{4+} + R \quad \textbf{[11]}$$

$$Cr^{4+} + RH^- \rightleftharpoons Cr^{3+} + RH^{-*} \quad \textbf{[12]}$$

Although Cr^{3+} may be less toxic (also not clearly established), many of the oxidized products produced will have negative effects of their own. For example, an *in vitro* study by Stearns and Wetterhahn demonstrated that dehydroascorbate is able to react with excess Cr^{6+}, producing Cr^{5+} and Cr^{4+} reaction intermediates such as adducts and/or radicals (28). These intermediates have been shown to induce pBR322 plasmid DNA strand breaks (28). This reaction was pH dependent, with higher incidents of breakage at pH values of 3.8 (28). Moreover, Cr^{3+} also result in DNA strand breakage at pH values between 6.0 and 8.9 (38), and so even the reduced chromium species are capable of genotoxic effects. In the presence of H_2O_2, this reaction can result in the formation of hydroxyl radicals and direct binding between Cr^{3+} and DNA, resulting in DNA adducts (38).

1.6 DNA Damage

In vitro studies have been a useful method to show how Cr^{6+} is able to cause DNA damage. Cr^{6+} is a known human carcinogen, however, it is suggested to not be the species directly responsible for the DNA damage (39). As previously discussed, the biological reduction of Cr^{6+} results in Cr^{5+}, Cr^{4+} and finally Cr^{3+} species. Cr^{5+} has been suggested to be the main species responsible for the

carcinogenic effects of chromium (31, 39). This is significant because it has been shown by other researchers that Cr^{5+} intermediates can be produced by a single electron reduction of Cr^{6+} within the liver of mice (17, 40). Also, it was shown that Cr^{5+} was the majority species found in the livers of mice treated with Cr^{6+} (17, 40). However, this does not mean that Cr^{6+} is not cause for concern, as it is the likely source of all Cr^{5+} within biological systems. Furthermore, Cr^{5+} is able to induce oxidative DNA cleavage, and/or nucleotide cleavage, at physiological pH values (pH 7.4) by hydrogen atom transfer from a deoxyribose ring, facilitated by H-bond formation with an oxo group of chromium complexes (31, 41). In addition, studies have shown that systems comprised of O_2 as well as Cr^{6+} and glutathione or Cr^{6+} and ascorbate, will generate a similar DNA damage result, to what is found in cell cultures of living organisms exposed to Cr^{6+} (31). This damage profile includes DNA strand breaks, alkali-labile sites and Cr^{3+} DNA adducts (31).

1.7 Supplemental Chromium

Chromium is thought to be an essential dietary nutrient (4, 7, 10, 11, 42). Within the body, its role is not fully understood, however the general consensus is that it plays a role in increasing insulin sensitivity (11, 42). Insulin is a hormone with myriad effects, ranging from increasing glucose uptake in muscle and fat, to stimulating cell growth and proliferation (43). Its most notable function is the regulation of blood glucose levels (43). Glucose uptake is initiated by the binding of insulin to the extracellular α-subunit of the insulin receptor (IR) on the cellular membrane (44, 45). Insulin binding to the α-subunit triggers the autophosphorylation of the intracellular β-subunit of the IR, activating the intracellular tyrosine kinase domain of the IR (44, 45). When activated, the IR phosphorylates multiple tyrosine residues on the downstream docking proteins insulin receptor substrate 1 and 2 (IRS-1 and IRS-2) (44, 45). Tyrosine phosphorylation of IRS-1 and IRS-2 facilitates their binding to the Src-homology 2 domains, resulting in the association between IRS-1 and the p85 regulatory subunit of phosphatidylinositol 2-kinase (PI3K) (44, 45). This results in

the recruitment of the p110 catalytic subunit of PI3K to the plasma membrane, causing the conversion of phosphatidylinositol-4,5-bisphosphate to phosphatidylinositol-3,4,5-triphosphate (44, 45). The summation of these reactions leads to the phosphorylation of protein kinase B (Akt) by PI3-dependent kinases (44, 45). The activation of Akt phosphorylates multiple downstream effectors, including Rab-GTPase activating protein, which eventually results in the translocation of glucose transporter-4 (Glut-4) vesicles from the cytoplasm to the cell surface, thus regulating cellular glucose uptake (44, 45). In addition, Akt also phosphorylates glycogen synthase kinase-3 to stimulate the formation of glycogen (44, 45). One proposed mechanism of how chromium becomes involved with the insulin signalling cascade within the body is shown in Figure 1.1 (44). Chromium enhances the kinase activity of IR-β, to increase the activity of downstream effectors of insulin signaling PI3K and Akt and to enhance Glut-4 translocation to the cell surface (44). Furthermore, chromium also down-regulates protein tyrosine phosphate-1B (PTP-1B) (the negative regulator of insulin signaling) and alleviates endoplasmic reticulum stress within the cells, preventing IRS from c-Jun N-terminal kinase (JNK)-mediated serine phosphorylation and subsequent ubiquitination (44). Because IRS was not phosphorylated by tyrosine, IRS can no longer function within the insulin signalling pathway (44). In addition, chromium activates the transient up-regulation of 5' AMP-activated protein kinase (AMPK), which leads to increased glucose uptake by the cell (44). Finally, chromium can mediate cholesterol efflux from the membranes by up-regulating sterol regulatory element-binding proteins responsible for controlling cellular cholesterol balance, causing Glut-4 translocation to the cell membrane and glucose uptake (44).

Another proposed mechanism of action for chromium within the body involves the chromium-binding oligopeptide chromodulin, which enhances insulin binding activity, and is depicted in Figure 1.2 (46, 47). This mechanism is initiated by insulin binding to the IR (46, 47). This results

in the stimulation of chromium uptake from blood into the cell (46, 47). The Cr^{3+} then binds to apochromodulin, forming chromodulin (holochromodulin) (46, 47). Holochromodulin is then able to bind to the IR, upregulating IR receptor kinase activity (46, 47). Finally, once blood insulin concentration drops, holochromodulin is released from the cell, reversing its effects (46, 47).

1.8 Plasma Proteomics

Proteomics is the study of proteomes and their function. A proteome is the entire make up of proteins expressed by an organism, tissue, or a cell. Blood sampling allows for the analysis of blood plasma for changes in the proteome of an organism to be measured. Only the plasma is used because blood travels the entirety of an organism and picks up proteins from different body systems along the way. Those proteins are found in the blood plasma. A single blood plasma sample can contain thousands of proteins (48). Changes in these proteins gives us a snapshot of the health of an organism and can tell us how they are affected by external stressors, such as chemical exposure or temperature changes, based on whether they increase or decrease in abundance. These changes are measured using a LC-MS/MS. The proteins are ionized (electrospray ionization) and then filtered by mass. The abundance is then measured as intensity values that are used to generate mass spectra data that is used to determine the probable sequence of the peptides. These peptide sequences are then searched against a database of known sequences to match them to proteins. Lastly, biological and molecular functions of these protein then allow us to determine the effect that the external stressor has on the organism.

1.9 Study Goals and Objectives

The goal of this study is to better understand the difference in effect of chromate, chromite, and chromium picolinate, on rainbow trout. The use of proteomics allowed us to determine the relative effects of Cr^{6+} to Cr^{3+}. Protein abundance in the blood plasma of the chromium exposed fish was

measured and compared to controls. This gave us an understanding of the differences in effect Cr^{6+} and Cr^{3+} have on the fish. A micronucleus assay was used to measure the DNA damaging effects that are associated with chromium exposure and served as the phenotypic anchoring for this study. Phenotypic anchoring provides us with observable effects to support changes we may see from proteomic analysis of blood plasma. The micronucleus assay was an ideal assay for this study, as the red blood cells in fish are nucleated, allowing for abnormalities of the cells nuclei to be easily observed with minimal preparation. Concurrently, we identified potential biomarkers to distinguish between Cr^{6+} and Cr^{3+} exposure. This was done by selecting proteins that had a significant change in abundance from the exposure and are associated with an adverse outcome correlated with chromium exposure. Furthermore, we also determined whether chromium picolinate has a beneficial or harmful effect in rainbow trout. The insulin sensitizing effects of chromium picolinate were measured against metformin HCl by inducing a blood glucose spike and testing the blood glucose concentrations of the rainbow trout. Plasma proteomics was also performed to compare chromium picolinate exposure, to that of inorganic Cr^{6+} and Cr^{3+}.

1.10 Figures and Tables

- PTP-1B = Protein Tyrosine Phosphate 1B
- IRS = Insulin Receptor Substrates 1 & 2
- ER = Endoplasmic Reticulum
- Ser = Serine
- PKB = Protein Kinase B (a.k.a. Akt)
- AMPK = 5' AMP-activated protein kinase
- Glut-4 = glucose transporter type 4

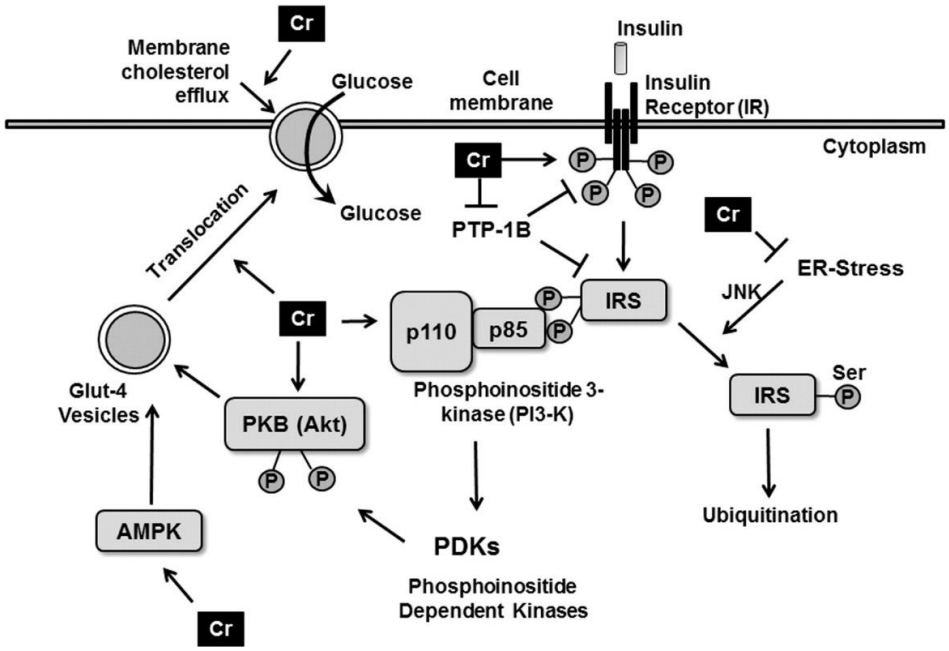

Figure 1.1. A proposed mechanism of how Cr^{3+} interacts within the Insulin signalling cascade by Hua et al. (44)

- InR = Insulin Receptor
- In = Insulin

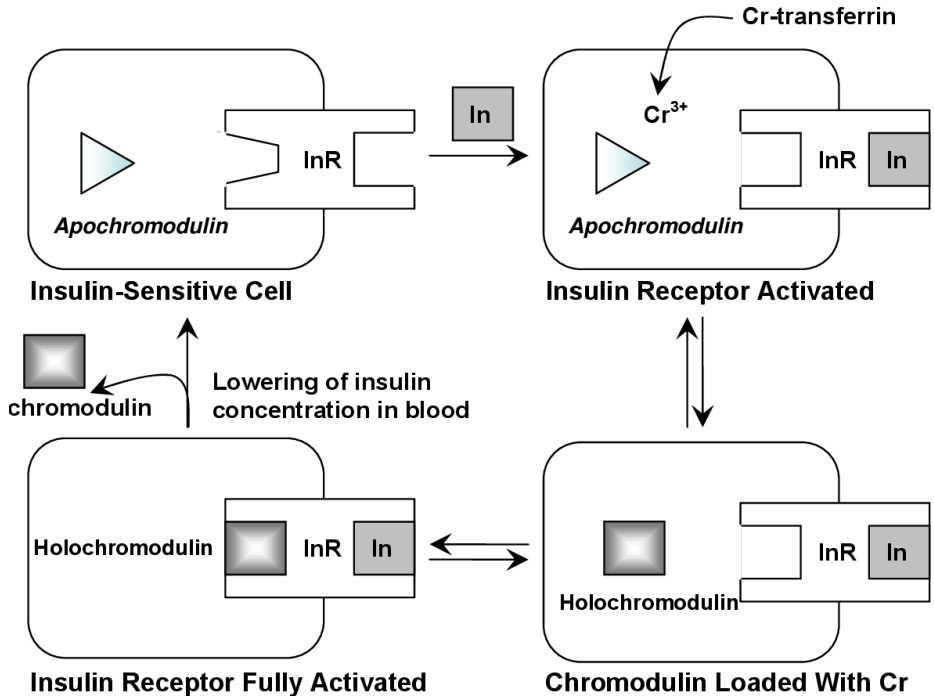

Figure 1.2. A proposed mechanism for the effects of Cr^{3+} on insulin signalling by Vincent JB (46, 47).

Chapter 2. Materials & Methods

2.1 Exposures and Assay Design

Rainbow trout (*Oncorhynchus mykiss*), ranging between 150 – 350 g were used as the model organism for this study. This species is specifically useful for this type of study because they are a widely accepted toxicological cold-water test species. Also, their size being ≥100 g allows for adequate volumes of blood (≥1 µL/g) to be collected. Furthermore, the rainbow trout proteome is fully sequenced, allowing for efficient and accurate protein identification. Lastly, they are a species that are native to North America and are a prized catch for both sport fishing and consumption. The fish for this study were purchased from Linwood Acres Trout Farms Ltd in Campbellcroft, Ontario. Upon reception of the fish, they were subjected to a two-week acclimation period. A maintenance diet of 45 g of Corey4 pellets, every other day, to prevent further growth.

The Aquatics Omics Lab houses twelve 1000 L flowthrough tanks, outfitted to run with both 12˚C and 25˚C water. Ten of the tanks were used for this study. Each tank housed 20 fish, totaling to 200 rainbow trout. Each tank was set up for five complete turnovers per day. Therefore, 5000L of water passed through each tank per day. The hourly flow rate was set to 208.33 L/Hour, which is an important metric for determining the contaminant dosing concentrations later on. Each tank is also outfitted with a manual standpipe, that was pulled daily, for approximately 30 seconds, to drain any waste produced by the fish. The fish experience a photoperiod of 16 hours light and 8 hours of darkness.

A 205U/CA Multi Channel Cartridge Watson-Marlow Bredel Pump was used to dose all ten tanks. Tubing (Code: Yellow/Yellow) with a bore size of 1.42 mm, and a flow rate range of 0.040 mL/minute at 0.5 rpm, to 7.2 mL/minute at 90 rpm was used. The flow rate selected for this study was 0.088 mL/min at 1.1 rpm (5.28 mL/Hour). This flow rate was verified by running the pump

with water and monitoring the hourly flow rates of the tubing connected from the concentrated contaminant bottles to the pump, and then from the pump to each of the ten tanks eductors that circulate the water around the tanks evenly. After the weekly measuring, the actual flow rate was determined to be 5.2 mL/Hour. At a flow rate of 5.2 mL/Hour, each bottle would last approximately 8 days.

All of the different chemical treatments were dispensed from opaque HDPE bottles into the tanks by the peristaltic pump. Because a flow through system was used, concentrated stock solutions for each contaminant had to be made and were individually dispensed to each tank. The exposures were performed in two groups, an inorganic chromium assay and a nutritional supplement assay. The inorganic chromium assay was set up as follows: Negative Control [0 µg/L], Low Potassium Chromate Concentration [0.02 µg/L], Medium Potassium Chromate Concentration [0.2 µg/L], High Potassium Chromate Concentration [20 µg/L], Low Chromium (III) Acetate Concentration [0.02 µg/L], Medium Chromium (III) Acetate Concentration [0.2 µg/L] and High Chromium (III) Acetate Concentration [20 µg/L]. The nutritional supplement assay was set up as follows: Negative Control [0 µg/L + 300 mL DMSO], a Chromium Picolinate Group [20 µg/L + 300 mL DMSO] and a Metformin Group [20 ppm]. The treatments were split into two groups because chromium picolinate needed to be dissolved in DMSO in order to make the stock solutions, and blood glucose concentration was being measured for both chromium picolinate and metformin. Therefore, a separate Negative control was required. An overview of the exposures can be found in Tables 2.1 and 2.2. The concentrations for the concentrated stock bottles were calculated by determining the dilution factor (DF) for the tanks (DF = Chemical Flow Rate/(Chemical Flow Rate + Water Flow Rate)). All of the stock bottle concentrations can be found in Table 2.3.

2.2 Chromium Exposure Solutions

Potassium chromate (CAS# 7789-00-6), chromium (III) acetate hydroxide (CAS# 39430-51-8), chromium picolinate (CAS# 14639-25-9), metformin hydrochloride (1,1-dimethylbiguanideine hydrochloride; CAS# 1185166-01-1), and DMSO (dimethyl sulfoxide; CAS# 67-68-5) were all purchased from Sigma-Aldrich (Oakville, Ontario, Canada).

Each of the highest concentration solutions were made in the following way. All glassware was rinsed with deionized water (DI) three times before use. Approximately 801.3021 mg of each of the previously mentioned chemicals was measured and transferred to a 1L beaker. The weigh boat was rinsed into the beaker with DI, and then approximately 900 mL of DI was added to the beaker. The solution was mixed with a stir bar for 5 minutes and then transferred to a 1L volumetric flask. The beaker was also rinsed three times with small volumes of DI into the volumetric flask. The flask was then diluted to one liter and was inverted 5 – 10 times. For the medium concentration solutions, 10 mL of the highest concentration solution was transferred to a clean 1L beaker, and all steps were repeated. For the low concentration solutions, 1 mL of the highest concentration solution was transferred to a clean 1L beaker, and all steps were repeated. For the chromium picolinate solution, the measured chemical was first dissolved in 300 mL of DMSO in a 1L beaker and stirred for 5 minutes. The volume was then increased incrementally by 150 mL with DI, stirring for 5 minutes between each addition, until 900 mL was reached. The solution was then added to a 1L volumetric flask and diluted to 1L. The chromium picolinate solutions were left overnight to ensure precipitation did not occur. All other solutions were immediately transferred to a 1L opaque HDPE Nalgene bottle for tank dosing.

2.3 Chromium Concentration and Speciation Measurements

2.3.1 Total Chromium Samples

The following summary of the water test methodology was completed by Lescord et al. at Laurentian University (shipped and delivered within 24 hours). A full detailed breakdown of the analysis can be found in Appendix B. Five samples for total chromium were taken, one from each of the experimental tanks, by adding 25 mL of tank water to a 50 mL falcon tubes. The five 20 µg/L and 0.2 µg/L tank samples were acidified using trace -grade HNO_3 to a concentration of 1% acid (360 µL in 25 mL of sample water; 67-70% purity, Fischer Chemicals™) immediately upon arrival. Samples were stored in the refrigerator overnight and analyzed for total chromium (and other elements) the following day on a Perkin Elmer® NexION 1000 inductively coupled plasma mass spectrometer (ICP-MS) under dynamic reaction cell (DRC) and kinetic energy discrimination (KED) detection modes. KED and DRC were used to remove any polyatomic interferences that may have been present; results between the two modes were in good agreement (data not shown) and DRC results are presented here, at the recommendation of industry professionals.

2.3.2 Chromium Speciation Samples

To assess the speciation of chromium in the various treatments, samples of tank water were preserved by adding sodium hydroxide (NaOH, to a concentration of 50 mM), sodium carbonate (Na_2CO_3, to a concentration of 28 mM), and ethylenediaminetetraacetic acid (EDTA, to a concentration of 10mM). To achieve the desired molarities, 0.05 g of NaOH (Fisher Chemicals A.C.S. Certified, 97.4%), 0.075 g of Na_2CO_3 (Fisher Chemicals Enzyme Grade, 99%), and 0.05 g of EDTA (Fisher Chemicals Electrophoresis Grade, 99%) were added to 25 mL of tank water in 50 mL falcon tubes. The resulting samples had an elevated pH (>11), which stabilized any Cr^{6+} present and prevented it from reducing into Cr^{3+}. Simultaneously, the added EDTA readily

complexed with the Cr^{3+}, stabilizing it and preventing oxidation into Cr^{6+}. Together, these effects helped to limit interconversion between Cr^{3+} and Cr^{6+} after sampling and before analysis. After the reagent additions, samples were gently inverted 5-10 times and heated using a Cole-Parmer sonicator at 60˚C for 60 minutes to speed-up the EDTA- Cr^{3+} complexation. Samples were cooled to room temperature, packed in with ice packs, and shipped overnight for analysis.

All preserved samples were analyzed for chromium speciation at the Purdue Central Analytical Facility at Laurentian University within 24-hours of collection. Sample were injected into an Metrohm® 940 Ion Professional IC Vario ion chronography (IC) system, equipped with a Metrosep Supp4 chromatography column (Metrohm®) to separate Cr^{3+} from Cr^{6+}. Species were eluted from the column using a 2 mM EDTA eluent (pH raise to 10.1-10.5 using NH_4OH) and detected using the Perkin Elmer® NexION 1000 ICP-MS. Detection was performed in DRC mode. The MDLs and limits of quantification (LOQs) were estimated to be 0.1±0.03 and 0.3±0.08 for Cr^{3+}, respectively, and 0.1±0.03 and 0.2±0.10 for Cr^{6+}, respectively. Detected counts per second (CPS) were compared against a linear calibration curve ($R2 > 0.9999$ for both Cr^{3+} and Cr^{6+}). The percentage of deviation from expected concentrations of all calibration standards were between -9.2 to 16.7% across both chromium species. It should be noted that at the time of writing, this method is experimental, and the results should be interpreted with caution.

Several QAQC tests were also performed during IC-ICP-MS speciation analysis. First, each tank was sampled and preserved twice and the percentage difference between these method duplicate samples was 12.1% for the 20 ng/mL Cr^{3+} tank and -1.7% for the 20 ng/mL Cr^{6+} tank; no Cr^{3+} or Cr^{6+} was detected in either of the 20 ng/mL picolinate samples. Second, the 20 ng/mL Cr^{3+} and Cr^{6+} samples were retested 5-days after collection and preservation, with the retested results being -12.5% and -9.2% different when compared to the initial values. A duplicate injection of the 20

ng/mL Cr^{3+} tank sample was also performed as an instrument duplicate, and it was 5.6% different from the original value. A second duplicate of this samples was also spiked at 5 ng/mL Cr^{3+} and Cr^{6+}, with 97.5% and 96.0% of the chromium recovered for the two species, respectively. Ongoing precision replicates (OPRs), with 1 ng/mL of Cr^{3+} and Cr^{6+}, were analyzed in the middle and end of the analytical run; 99.5% and 99.4% of Cr^{3+} and 102.8% and 104.2% of Cr^{6+} was recovered from these two tests. Throughout the analysis, four eluent blanks were also analyzed as instrument blanks, and no Cr^{3+} or Cr^{6+} was detected in any of these samples. Similarly, two method blanks (distilled (DI) water and MilliQ water) were preserved using the same method as samples and analyzed for Cr^{3+} and Cr^{6+} and neither chromium species was detected using IC-ICP-MS. Lastly, three tank samples, the 20 ng/mL Cr^{3+}, Cr^{6+}, and picolinate, and the two blanks samples (DI water and MilliQ water) were analyzed for total chromium by diluting 1 mL of sample in 9 mL of 1% HNO_3. ICP-MS analysis was performed following the same methods described in section 2.3.1 and the results were in good agreement with the speciation results (Table 2.4). It is noteworthy that despite no detection of Cr^{3+} or Cr^{6+} in speciation analysis, 0.4 to 0.9 ng/mL total chromium was detected in the DI and MilliQ blanks across the three analytical runs. However, no blank subtractions were applied to samples because the speciation of the chromium was unknown.

2.4 Metformin Concentration Measurement

Two 25 mL replicates of the 20 µg/L tank water were collected in 50 mL conical tubes. These samples were injected onto a HILIC zwitterion column (Agilent InfinityLab Poroshell 120 HILIC-Z, 2.1 × 150 mm, 2.7 µm, PEEK lined) and then separated using the 1260 Agilent Liquid Chromatography system with the. Agilent 6545 Accurate-Mass Quadrupole Time-of Flight (Q-TOF) mass spectrometer as the detector, along with 5, 10X serial diluted metformin HCl standard solutions. Samples were separated with a gradient using solvent A (95% H_2O 5% acetonitrile and

0.1% formic acid) and Solvent B (5% H_2O 95% acetonitrile and 0.1% formic acid) as described in Appendix A). A standard curve was made with five calibration points, and the concentration of metformin in our tank water was determined from the standard curve. The final concentration for metformin can be found in Table 2.2.

2.5 Fish Tissue and Blood Sampling

The fish in each tank were exposed to the chromium solutions, metformin, or solvent control for 28 days. After the exposure period, the fish were weighed, fork lengths measured, and then blood was sampled from each fish by caudal puncture. The fish were sedated using electrofishing gloves. This method was used instead of traditional chemical sedation, because the anesthetic that is normally used in the Aquatic Omics Lab (Tricaine methanesulfonate (MS-222), 135 mg/L) interferes with the normal function of the ion-channels in pancreatic β-cells (49). This would result in an increase in blood glucose, and in an inaccurate glucose reading. Electro-sedation was employed instead using fish handling gloves that apply a continuous low-voltage direct current across the body of the fish. The blood was collected in heparinized vacutainers. A portion of this blood was used to measure the glucose levels of each fish using a portable One Touch Ultra strip reader. The strip was inserted into the strip reader, and then simply touched against the tip of a plastic 2 mL pipette, to record the glucose reading. Another portion of blood was used for a micronucleus assay, according to the protocol outlined by Hussain et al. (50) . The remaining portion of blood was centrifuged (2000 rpm for 10 minutes) to collect blood plasma for proteomic analysis. All the fish were euthanized post-blood sampling by MS-222 immersion. After sacrifice, the fish were dissected to collect livers and fillets that were flash frozen in the vapour phase of liquid nitrogen and stored at -80˚C. All of the liver samples were weighed and then cut into left and right lobes and frozen separately. The liver weights were used to calculate the hepatosomatic

index (HSI). This is done by dividing the mass of the liver by the total mass of the fish. Both the liver and fillet samples will be used to analyze chromium tissue accumulation and speciation sometime in the future.

2.6 Micronucleus Assay

Immediately after caudal vein puncture, clean microscope slides were smeared with blood and promptly fixed in methanol for 3 minutes (CAS# 67-56-1). Two slides were smeared per fish (400 slides total). The slides were then air dried at room temperature (23˚C) for 20 minutes. Next the slides were stained with 100% Giemsa solution for 1 minute, then rinsed with DI and left to air dry completely at room temperature. The slides were stored in slide boxes until they were needed for imaging.

Cells were observed at 1000x magnification using immersion oil on a Leica DM E compound light microscope, with a cell phone adapter to take pictures. Ten full field of view photos were taken per slide (~1000 cells) for a total of 4000 photos. Cells were scored as either "Normal" or "Abnormal". Abnormal cells fell into the following categories: notched (NT), blebbed (BL), lobbed (LB), binucleated (BN) (50-52). Only notched and binucleated cells were observed in this study. Figure 2.1 shows an example of each nuclear abnormality. The results are expressed as a percentage of the total number of cells observed (Number of Abnormal Cells / Total number of cells). The total cell count was automated using Image-Pro 10. The abnormality cell count was done manually through visual inspection of the photos.

2.7 Plasma Proteomic Analysis

Plasma samples were thawed on ice for 30 minutes. Once thawed, the plasma was vortexed and then 15 μL of each sample was added to a 1.5 mL microcentrifuge tube. Next, 35 μL of 200 mM

AB buffer and 2.65 µL of 100 mM TECP buffer were added to the same tube. This solution was vortexed for 5 seconds and then left to incubate at room temperature for 45 minutes. After incubation, 2.8 µL of 200mM IAA in 200 mM AB buffer was added. The solution was vortexed again, and then incubated at room temperature for 45 minutes in the dark. At the end of the dark incubation period, 50 µL of 20% (v/v) formic acid (Fisher Scientific: A118P-500) in Milli Q water was added. Lid locks were placed on each tube, and then incubated at 115˚C in a heating block for 30 minutes (VWR 96 place heating block). After the final incubation, the samples were cooled outside of the heating block for 1 minute and then placed, lids open, in a Savant SpeedVac Centrifugal Evaporator, to be evaporated to near dryness (~20 µL). The samples were then reconstituted with 20 µL of HPLC dilution buffer A1 (94.9% Milli Q water, 5% HPLC optima grade Acetonitrile (Fisher Scientific), 0.1% Formic acid), and vortexed gently for 2 minutes. Once the dried samples were fully re-suspended, they were then centrifuged at 14 000 *xg* for 10 minutes to pelletize any debris. Then, 20 µL of supernatant was transferred to 2 mL HPLC vials with a 250 µL conical polypropylene spring bottom insert, and then capped with 9 mm blue PTFE/silicone/PTFE screw caps. Finally, the samples were stored at 4˚C until analysis on our Agilent 6545 Accurate-Mass Quadrupole Time-of Flight (Q-TOF) mass spectrometer.

Samples were separated by reverse phase liquid chromatography using a Zorbax, 300SB-C18, 1.0 × 50 mm 3.5 µm column on a 1260 Infinity Liquid Chromatography system (Agilent Technologies Canada Inc., Mississauga, ON) with 2 µL injection volume. Separated peptides were detected by our Agilent 6545 QTOF mass spectrometer. Each sample was injected once. A blank and an analytical standard of digested bovine serum albumin (BSA) peptides were injected after every 10 samples.

Spectrum Mill MS Proteomics Software (Rev BI.07.07.213) was used to identify the peptide sequences from the spectral data and then search them against the Uniprot reference proteome (downloaded February 2019). Skyline (Version 20.2) software was used to determine protein abundances using chromatographic peak area and MS1 filtering to fill in missing values. The proteins were quantified at the MS1 level, using the DDA (Data Dependent Analysis) workflow in Skyline. A cut-off score of 0.9, 5 maximum missed cleavages, and retention time window of 5 minutes was used, using TOF transition settings and DDA acquisition method for MS/MS filtering. Mass Profiler Professional (MPP) (Version 15.1) software was used to import results from Skyline, and then export the data into a comma separated format that included all the UniProt accession numbers for proteins detected with protein abundance in total mean intensity for the peak areas of each protein-peptide group. The rainbow trout accession numbers were mapped to human ortholog gene symbols (HOGS) using a python script, to automatically BLAST the accession numbers against the human proteome and then find the orthologous human gene symbols using UniProt. Any unmapped gene symbols were mapped manually. After mapping, maximum values were used to consolidate the data set. Finally, all abundances that had a mean intensity value less than 5000 were removed.

Graph Pad Prism 9 (Version 9.1.2) was used to do the statistical analysis for the HSI, blood glucose concentration (BGC) and micronucleus assay data sets. The inorganic chromium assay (Control, $Cr^{3+}_{0.02\ \mu g/L}$, $Cr^{3+}_{0.2\ \mu g/L}$, $Cr^{3+}_{20\ \mu g/L}$, $Cr^{6+}_{0.02\ \mu g/L}$, $Cr^{6+}_{0.2\ \mu g/L}$ and $Cr^{6+}_{20\ \mu g/L}$) and the nutritional supplement assay (Control, Chromium Picolinate and Metformin HCl) were analysed separately. First, descriptive statistics were done for all treatment groups for both HSI and BGC. Next, a Shapiro-Wilk test was used on all treatment groups to test for normality. Only the HSI data sets passed for normality. The BGC data set was not normal and therefore, non-parametric tests were used for subsequent analysis. Then, an ordinary one-way ANOVA was used to analyse both

inorganic and nutritional supplement assay HSI data sets to determine if there were significant differences in comparison to the respective control groups ($p = 0.05$). Both were followed by Tukey's multiple comparisons tests to look for significant differences between the groups themselves. A Kruskal-Wallis test was used to analyse the blood glucose concentration data sets, followed by Dunn's multiple comparison test. The micronucleus data was analysed by making contingency tables using the micronucleus count data for all eight of the non-control treatment groups. A Fisher's exact test was then used to determine if there were significant differences compared to the control groups. Graph Pad was also used to generate all the figures for the aforementioned analyses.

The consolidated mass spectral data was imported to Mass Profiler Professional (MPP) (Version 15.1). The data was pareto-scaled, and then the inorganic chromium assay only, was filtered by abundance for entities where at least 100% of samples in any 2 out of 7 conditions have values >5000. An ANOVA was used to analyze proteins from the inorganic chromium and nutritional supplement assays ($\alpha = 0.05$). MPP was also used to generate all of the Venn diagrams. Enrichment analysis was then performed on the HOGS of significantly different proteins (p-value < 0.05), along with their log fold change values, using ConsensusPathDB-human(CPDB) to find pathways that display significant co-ordinated shifts in the associated gene abundance (53, 54). Graph Pad was used again to put together response curves for the HOGS of interest across all of the Group A treatments, using the averaged LC-MS/MS results.

2.8 Figures and Tables

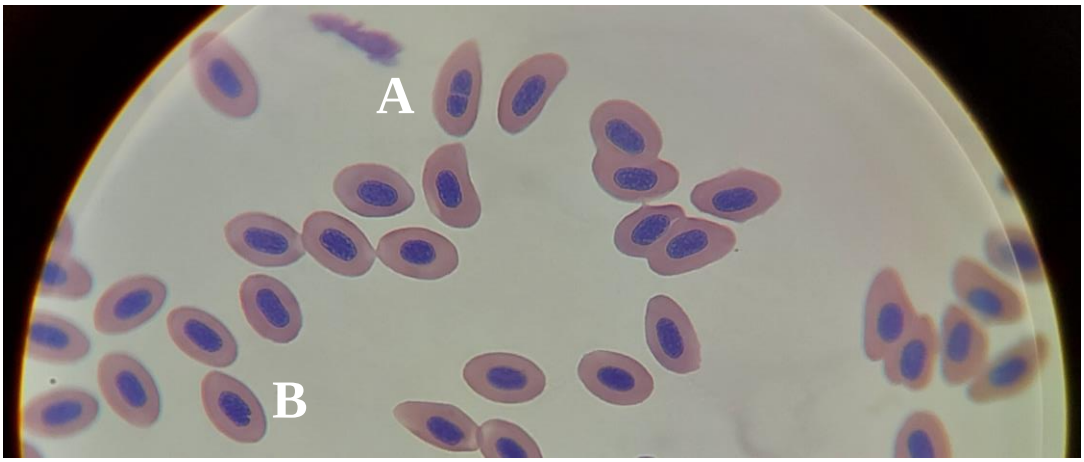

Figure 2.1. Rainbow trout red blood cells stained with Giemsa observed at 1000X under oil immersion. (A) Split nucleus. (B) Notched nucleus.

Table 2.1. Overview of the nominal and measured inorganic chromium assay concentrations.

Exposure	*Concentration (µg/L)*	
	Nominal	**Measured**
Control	0	0
Potassium Chromate ($Cr^{6+}_{0.02\ µg/L}$)	0.02	0.00985
Potassium Chromate ($Cr^{6+}_{0.2\ µg/L}$)	0.2	0.0985
Potassium Chromate ($Cr^{6+}_{20\ µg/L}$)	20	9.85
Chromium (III) Acetate ($Cr^{3+}_{0.02\ µg/L}$)	0.02	0.00844
Chromium (III) Acetate ($Cr^{3+}_{0.2\ µg/L}$)	0.2	0.0844
Chromium (III) Acetate ($Cr^{3+}_{20\ µg/L}$)	20	8.44

Table 2.2. Overview of the nominal and measured nutritional supplement assay concentrations.

Exposure	*Concentration (µg/L)*	
	Nominal	**Measured**
Control	0	0
Chromium Picolinate	20	<MDL
Metformin HCl	20	66.56

Table 2.3. Overview of each stock bottle used to dose each tank in both the inorganic chromium assay and the nutritional supplement assay.

Bottle	*Concentration (mg/L)*
Control (Inorganic Chromium Assay)	0
$Cr^{6+}_{0.02\ \mu g/L}$	0.8013
$Cr^{6+}_{0.2\ \mu g/L}$	8.0130
$Cr^{6+}_{20\ \mu g/L}$	801.3020
$Cr^{3+}_{0.02\ \mu g/L}$	0.8013
$Cr^{3+}_{0.2\ \mu g/L}$	8.0130
$Cr^{3+}_{20\ \mu g/L}$	801.3020
Control (Nutritional Supplement Assay)[1]	0
Chromium Picolinate[2]	801.3020
Metformin HCl	801.3020

[1]30% DMSO solution (300 mL DMSO in 1L of DI).

[2]In a 30% DMSO solution.

Table 2.4. Final Cr^{3+}, Cr^{6+} and Cr picolinate measured concentrations analyzed by ICP-MS. Supplemental information about the tank water chemistry is included.

	Tank information				*Measured chromium concentrations (ng/mL)*			
Exposure	**Temp (°C)**	**D.O. (mg/L)**	**Cond (µS/cm)**	**pH**	**[Cr(III)]**	**[Cr(VI)]**	**Total [Cr] (speciation)[3]**	**Total [Cr] (acidified)[4]**
Cr(III), 20µg/L	12.7	10	330	8.18	8.44[1]	ND[2]	11.37	11.37
Cr3(III), 0.2µg/L	13	8.7	331	8.09	NA	NA	NA	0.24
CrPic, 20µg/L	12.5	9.5	331	8.15	ND	ND	2.62	1.36
Cr(VI), 20µg/L	12.5	9.4	330	8.17	ND	9.85[5]	8.56	7.83
Cr(VI), 0.2µg/L	12.3	10.2	331	8.15	NA	NA	NA	0.25

[1]Duplicate sample = 7.35* ng/mL; re-analysis three days later = 9.57* ng/mL

[2]A rise in chromatographic baseline was identified as a peak, calculated at 0.156 ng/mL, but it was not considered a true detection; duplicate sample = ND; re-analysis three days later = ND;

[3]Speciation samples were also analyzed for total [Cr] by diluting the preserved sample 10x into 1%HNO_3 before ICP-MS analysis.

[4]Blank concentration = 0.45-0.98 ng/mL

[5]Duplicate sample = 10.02 ng/mL; re-analysis three days later = 10.8 ng/mL (during re-analysis a Cr(III) peak was also identified and quantified at 0.536 ng/mL, but this was due to a baseline interference)

Chapter 3. Results

3.1 Water Chemistry

Water from the tanks tested by Lescord et al. at Laurentian University, was determined to be approximately 50% of the nominal values. The 20 µg/L treatment groups measured approximately 10 µg/L. All of the 0.2 µg/L and 0.02 µg/L treatments ended up being <MDL (0.1 µg/L) for the species analysis, therefore the measured concentrations were estimated by assuming the concentration would be equivalent to the order of magnitude less than the measured 20 µg/L treatment groups. Thus, the 0.2 µg/L and 0.02 µg/L treatments ended up being approximately 0.1 µg/L and 0.01 µg/L respectively. Metformin ended up being approximately six times the expected concentration at 65 µg/L. All of the exact measured final tank concentrations can be found in Tables 2.1, 2.2 and 2.3.

3.2 Hepatosomatic Index (HSI)

Descriptive statistics for the HSI of both assays can be found in Tables 3.1 and 3.2. For both assays, the HSI the passed the Shapiro-Wilk test for normality ($\alpha = 0.05$). There were no significant differences in HSI between the treatments and the control after the inorganic chromium assay (One-way ANOVA, Tukey's HSD post-hoc test ($p > 0.05$)). For the chromium supplement assay, the one-way ANOVA suggested that there were no treatment effects on HSI ($p > 0.05$), however, Tukey's HSD post hoc identified a significant difference between the metformin and chromium picolinate treatment groups ($p < 0.05$). The results are displayed as violin plots in Figures 3.1 and 3.2.

3.3 Blood Glucose Concentration (BGC)

Blood glucose concentration data from the nutritional supplement assay failed the Shapiro-Wilk test for normality. Thus, we performed the non-parametric Kruskal-Wallis test on the BGC data

set, which identified significant differences between the control and treatment groups ($p < 0.05$). Dunn's multiple comparisons post hoc test revealed that there was a significant difference between the control and metformin HCl treatments ($p < 0.05$). No other comparisons resulted in a significant difference. Full statistics for the BGC results can be found in Table 3.3. The result is displayed as a violin plot in Figure 3.3.

3.4 Red Blood Cell Micronucleus Assay

All of the count and ratio data recorded for the micronucleus assay slides data can be found in Figures 3.4 and 3.5. The Fisher's exact test performed on the inorganic chromium assay treatments identified two significant differences ($p < 0.05$), between the inorganic chromium assay Control and $Cr^{3+}_{0.02\ \mu g/L}$ ($p = 0.0313$), and between the inorganic chromium assay Control and $Cr^{6+}_{0.2\ \mu g/L}$ ($p = 0.0073$). No significant differences in treatment were detected for cell abnormalities in the chromium supplement assay.

3.5 Plasma Proteins

A total of 2980 proteins were detected after filtering, among all of the treatments in the inorganic chromium assay. An ANOVA of the filtered inorganic chromium data set resulted in 66 proteins that were significantly different in abundance compared to control (Tukey's HSD post-hoc test, $p < 0.05$). Venn diagrams were used to visualize and compare the number of significantly different proteins in each treatment (Figures 3.6, 3.7, 3.8, 3.9 and 3.10). Figure 3.6 compares the proteins with different abundance from the control, between all three of the Cr^{6+} concentrations. This comparison resulted in 61 shared proteins between all three exposure groups. Figure 3.7 compares the proteins that are different from the control, between all three of the Cr^{3+} concentrations, with 56 proteins shared among all three exposure groups. Figure 3.8 compares the proteins that were different compared to the control, between $Cr^{6+}_{0.02\ \mu g/L}$ and $Cr^{3+}_{0.02\ \mu g/L}$ (62 shared proteins). Figure

3.9 compares the proteins that differed compared to control between $Cr^{6+}_{0.2\ \mu g/L}$ and $Cr^{3+}_{0.2\ \mu g/L}$ (55 shared proteins). Figure 3.10 compares the significantly different proteins from the control between Cr^{6+}_{20} µg/L and $Cr^{3+}_{20\ \mu g/L}$ (62 shared proteins). More than 80% of the proteins that were significantly different from the control treatment, were shared between both Cr^{3+} and Cr^{6+} exposure groups and across the low-medium-high concentration gradient for both chromium species.

A total of 4018 proteins were detected among all of the treatments in the chromium supplement assay, however, no significantly different proteins were identified in any of the treatments, compared to control. The enrichment analysis using Gene Ontology for the 66 significantly different proteins identified among the treatments from the inorganic chromium assay, did not identify any biological processes that were linked to known adverse outcomes or disease pathways that are associated with chromium exposure. The majority of the HOGS were associated with broad functional categories, such as response to stimulus (59%), multicellular organismal process (34.4%), and biological regulation (34.4%). A full breakdown of all of the pathways identified can be found in Figure 3.11. These results were similar for the gene ontology molecular function search, with the majority of HOGS associated with binding (32.8%), catalytic activity (32.8%), and molecular function regulation (9.8%), Figure 3.12.

The CPDB enabled a broader search and produced more nuanced results that contained specific information. As a starting point, we focused on the transition metal ion binding pathway because chromium is a transition metal. Trim21 was the only gene associated with any sort of notable adverse outcome. Specifically, Trim21 can be indicative of hepatocellular carcinoma which can be correlated to the hepatotoxicity of chromium. Other outcomes were not easily correlated to chromium and were also not easily correlated with other proteins involved in the pathway.

Therefore, we shifted focus to a less specific pathway, metal ion binding. Trim21 was also associated with this pathway. In addition, Rock2, Jak2, Slc8a1 and Flt1 were also identified to have notable adverse outcomes (see Table 3.4 for more detail). These five genes were all associated with circulatory system related biological processes. Figure 3.13 emphasizes the overlap of the five HOGS across different heart, blood vessel, circulatory and metal binding pathways. From the circulatory specific pathways, Myh4, Myh6 and Col22a1 were identified to have notable adverse outcomes associated with decreased abundance (Table 3.5). The full names and descriptions of the adverse outcomes related to the proteins can be found in Table 3.4 and Table 3.5. Furthermore, all eight of the HOGS identified were downregulated in comparison to the inorganic assay Control, which is also observed in the response curves for each protein (Figures 3.14.1 and 3.14.2). Other than the downregulation, no other pattern was identified. When the response curve was isolated for Cr^{6+} and Cr^{3+} only, a small increase, then decrease in protein abundance was observed with increasing concentration (Cr^{6+} - Figures 3.15.1, 3.15.2 and Cr^{3+} - Figures 3.16.1 and 3.16.2). For Cr^{3+}, this pattern of abundance is observed for the proteins Rock2, Trim21, Flt1, Myh4 and Col22a1, while for Cr^{6+}, this was observed for Myh6, Flt1, Myh4 and Col22a1.

3.6 Figures and Tables

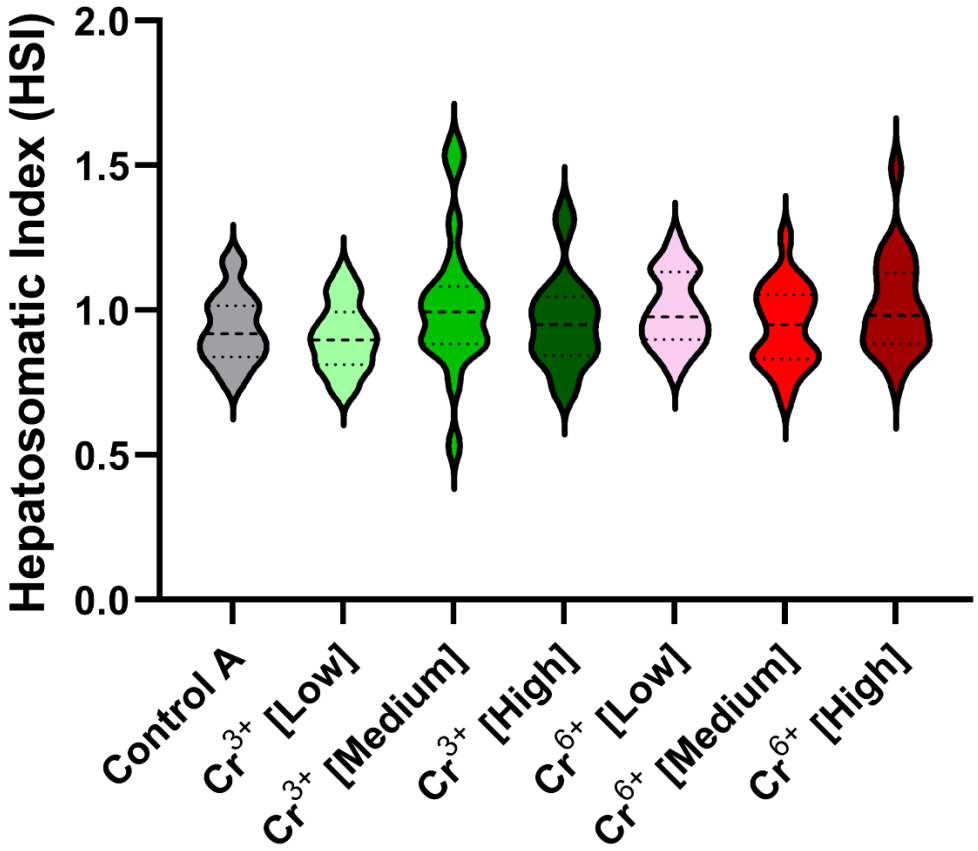

Figure 3.1. Violin plots of the hepatosomatic indexes (HSI) from rainbow trout exposed to different concentrations of chromium (III) acetate and potassium chromate (inorganic chromium assay (ICA)). A One-Way ANOVA was performed on this ICA data set. Chromium exposure resulted in no significant difference in HSI compared to Control, *p*-Values > 0.05. Tukey's HSD resulted in no significant difference between any of the treatment groups, at a 0.05 significance level.

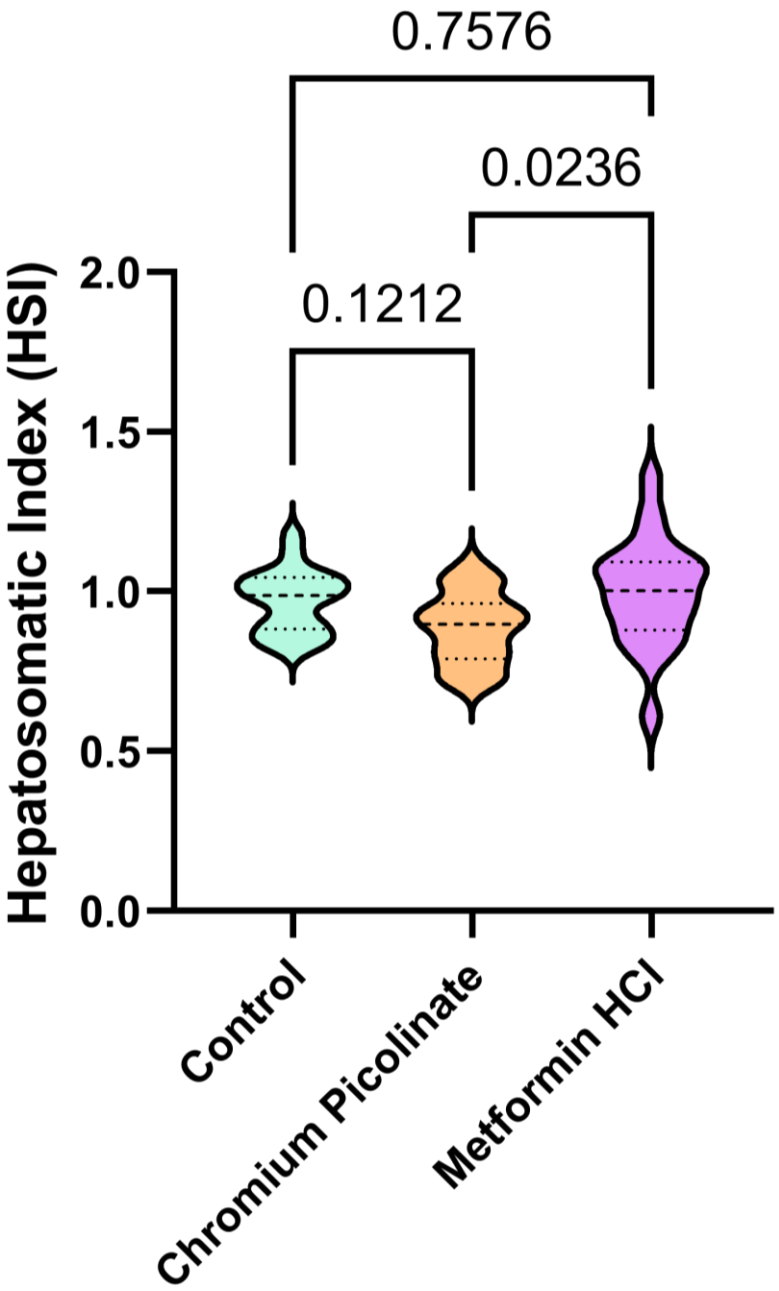

Figure 3.2. Violin plots of the hepatosomatic indexes (HSI) from rainbow trout exposed to chromium picolinate and metformin HCl (nutritional supplement assay (NSA)). A One-Way ANOVA was performed on this NSA data set. Chromium picolinate and metformin exposure resulted in no significant difference in HSI compared to Control, *p*-Value > 0.05. Tukey's HSD showed a significant difference between the chromium picolinate and metformin HCl treatments, $p < 0.05$. No other differences were identified.

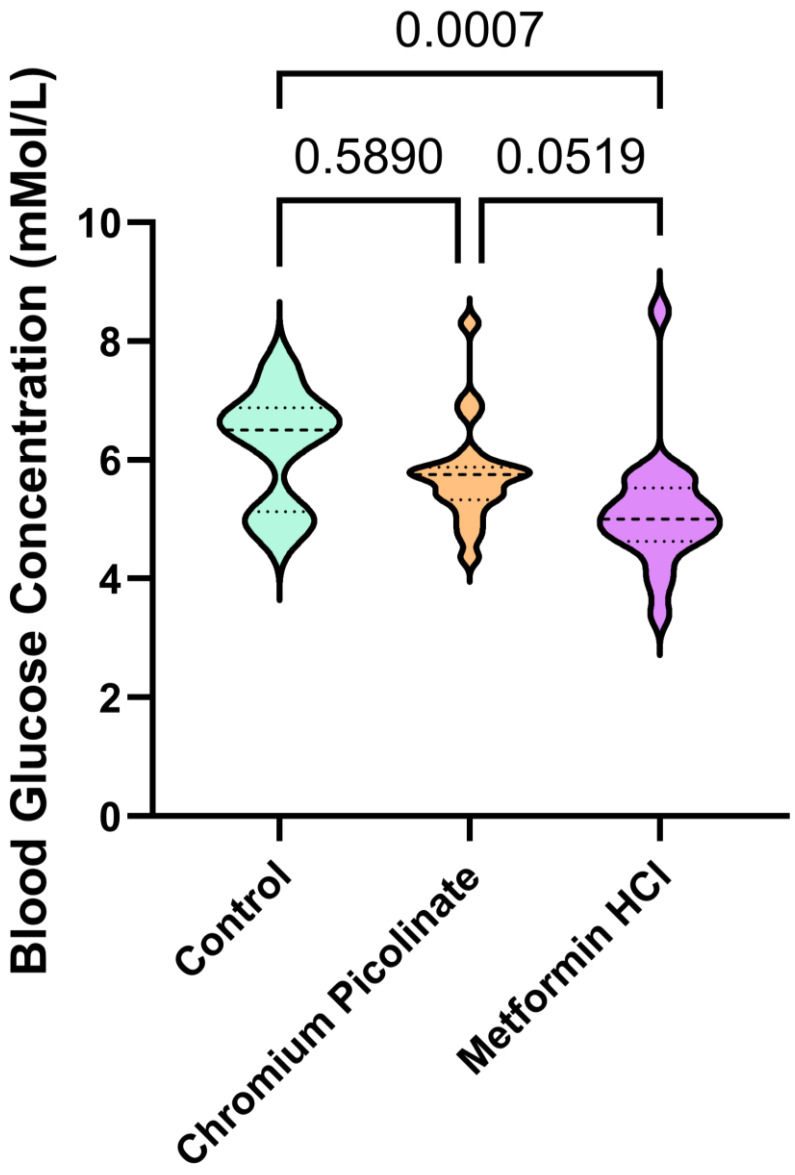

Figure 3.3. Violin plots of the blood glucose concentrations (mMol/L) measured from rainbow trout exposed to chromium picolinate and Metformin HCl, 30 minutes after feeding (nutritional supplement assay (NSA)). A Kruskal-Wallis test was performed on this NSA data set. Chromium picolinate and metformin exposure resulted in no significant difference between Control and the two treatments, *p*-Value > 0.05. Dunn's multiple comparisons test showed a significant difference between Control and metformin HCl only, $p < 0.05$.

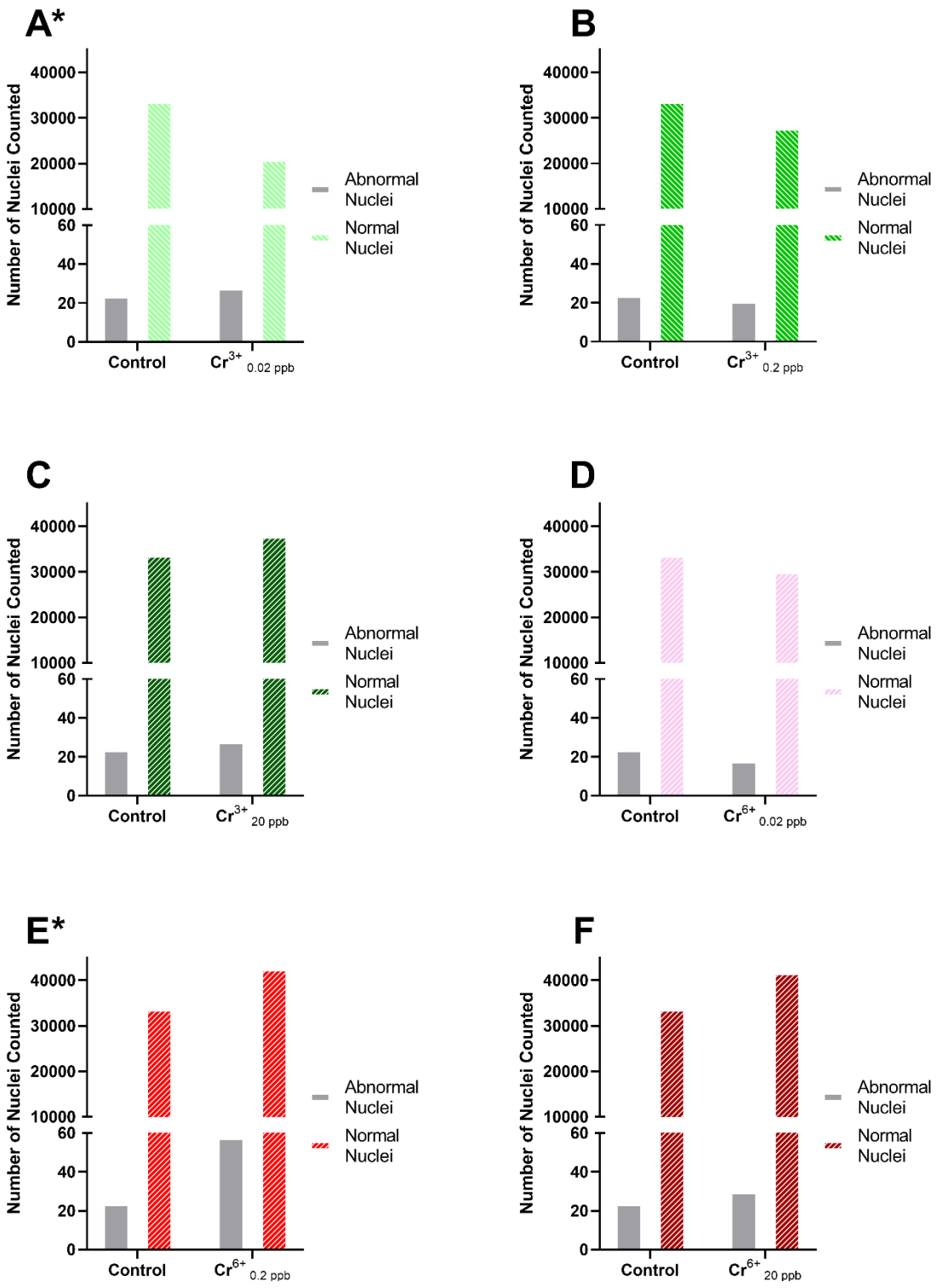

Figure 3.4. Cell counts from the micronucleus assay for the inorganic chromium assay. Each treatment was subjected to the Fisher's exact test and a 0.05 significance level. The treatments in graphs A and E (indicated by an asterisk) resulted in statistically significant difference compared to Control (p = 0.0313 and p = 0.0073 respectively)

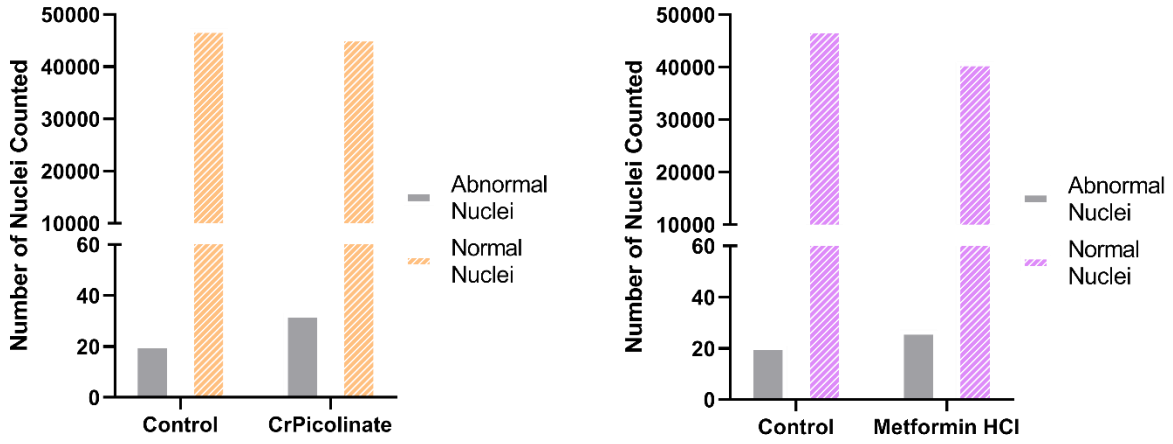

Figure 3.5. Cell counts from the micronucleus assay for the nutritional supplement assay. Each treatment was subjected to the Fisher's exact test and a 0.05 significance level. No treatments in these graphs resulted in statistically significant difference compared to Control.

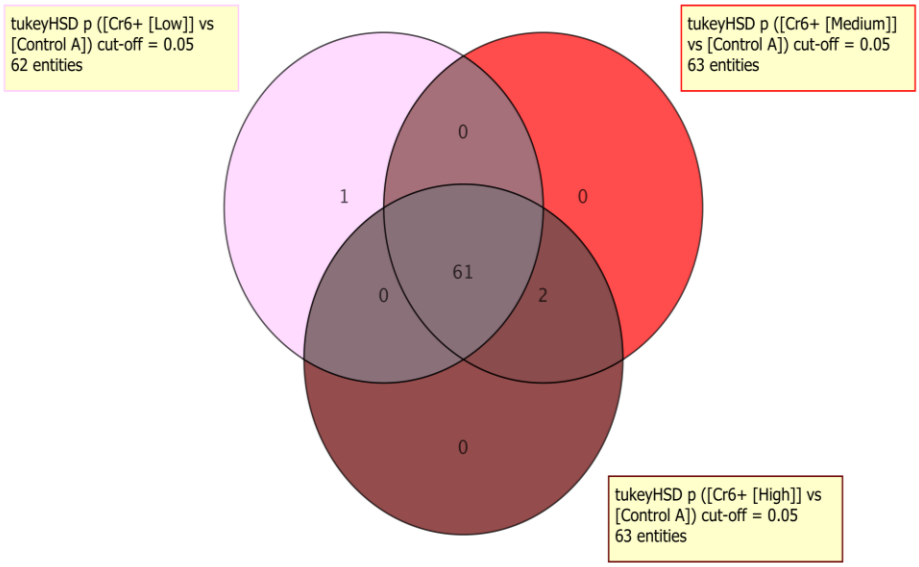

Figure 3.6. A Venn diagram of the significantly different proteins in rainbow trout blood plasma that resulted from a One-Way ANOVA and Tukey's HSD performed on the LC Q-TOF MS protein intensity values and the associated human gene symbols. This diagram compares significantly different proteins between $Cr^{6+}{}_{0.02\ \mu g/L}$ – Control, $Cr^{6+}{}_{0.2\ \mu g/L}$ – Control and $Cr^{6+}{}_{20\ \mu g/L}$ – Control.

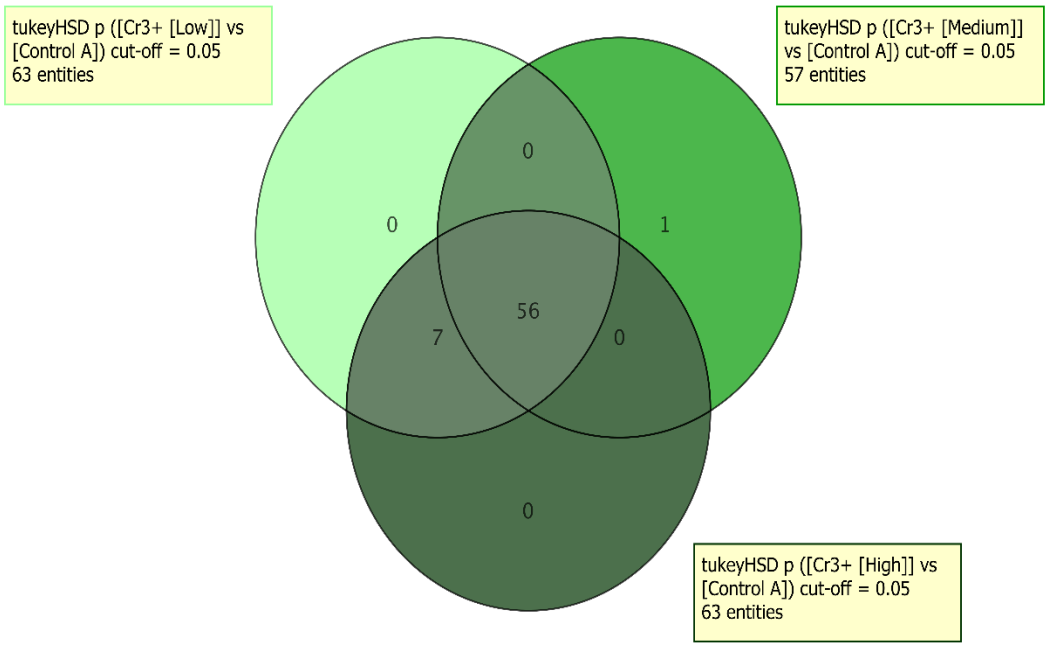

Figure 3.7. A Venn diagram of the significantly different proteins in rainbow trout blood plasma that resulted from a One-Way ANOVA and Tukey's HSD performed on the LC Q-TOF MS protein intensity values and the associated human gene symbols. This diagram compares significantly different proteins between $Cr^{3+}{}_{0.02\ \mu g/L}$ – Control, $Cr^{3+}{}_{0.2\ \mu g/L}$ – Control and $Cr^{3+}{}_{20\ \mu g/L}$ – Control.

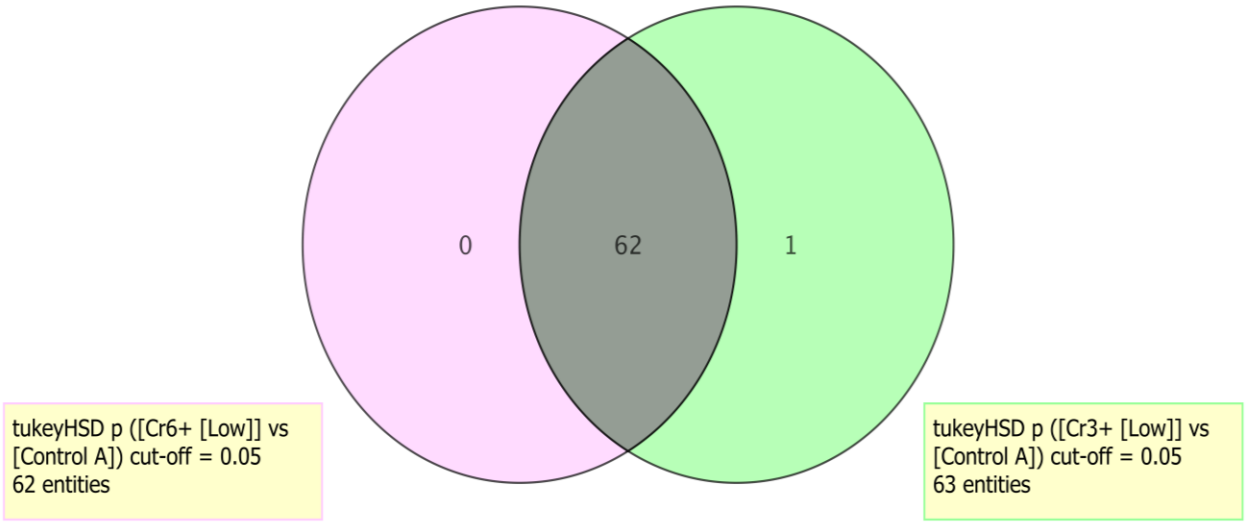

Figure 3.8. A Venn diagram of the significantly different proteins in rainbow trout blood plasma that resulted from a One-Way ANOVA and Tukey's HSD performed on the LC Q-TOF MS protein intensity values and the associated human gene symbols. This diagram compares significantly different proteins between $Cr^{6+}{}_{0.02\ \mu g/L}$ – Control and $Cr^{3+}{}_{0.02\ \mu g/L}$ – Control.

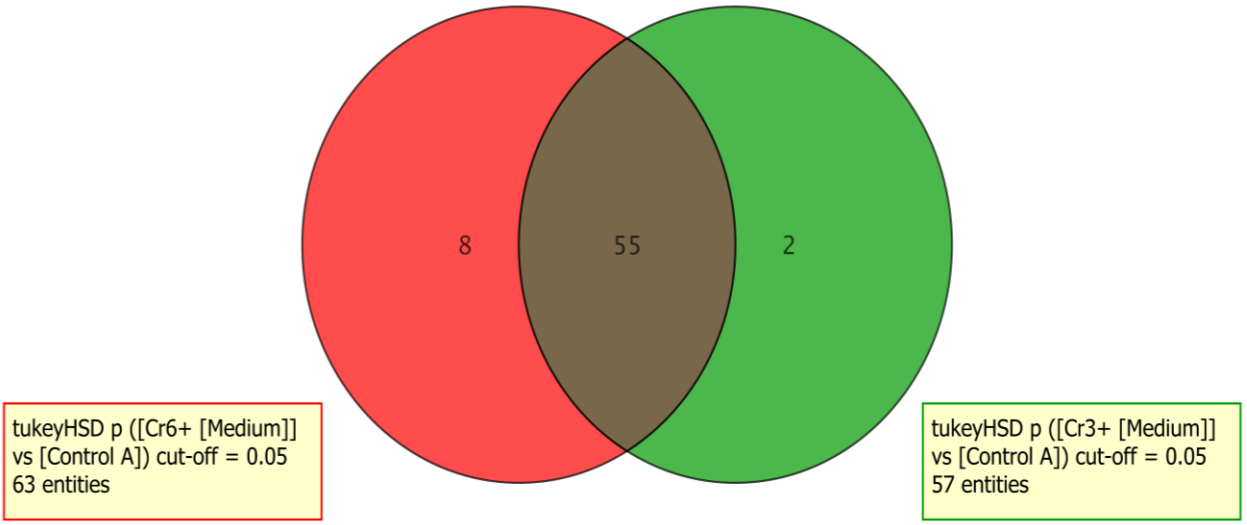

Figure 3.9. A Venn diagram of the significantly different proteins in rainbow trout blood plasma that resulted from a One-Way ANOVA and Tukey's HSD performed on the LC Q-TOF MS protein intensity values and the associated human gene symbols. This diagram compares significantly different proteins between $Cr^{6+}{}_{0.2\ \mu g/L}$ – Control and $Cr^{3+}{}_{0.2\ \mu g/L}$ – Control.

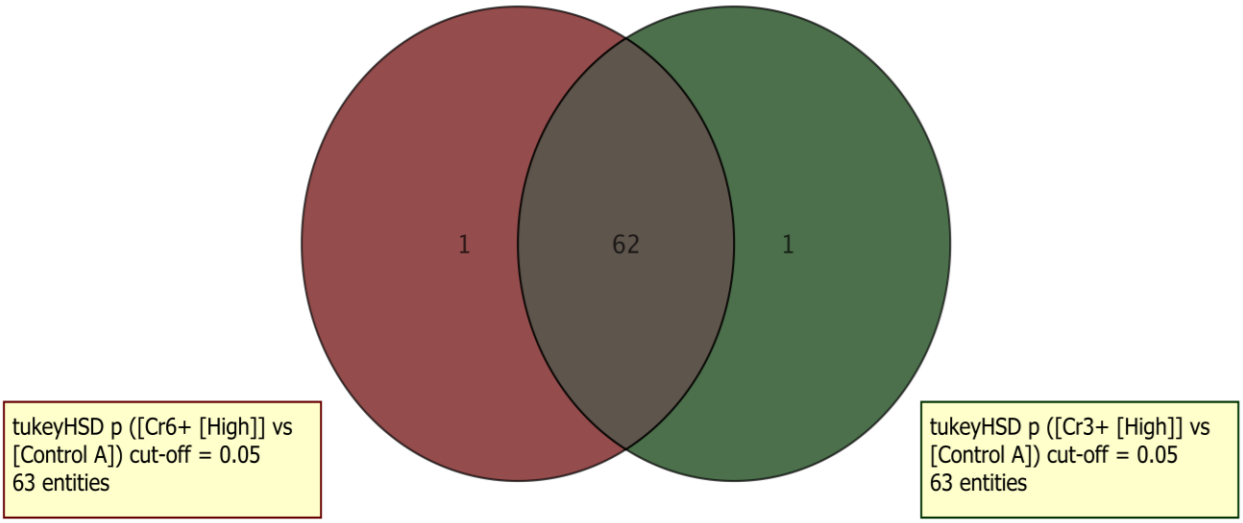

Figure 3.10. A Venn diagram of the significantly different proteins in rainbow trout blood plasma that resulted from a One-Way ANOVA and Tukey's HSD performed on the LC Q-TOF MS protein intensity values and the associated human gene symbols. This diagram compares significantly different proteins between $Cr^{6+}{}_{20\ \mu g/L}$ – Control and $Cr^{3+}{}_{20\ \mu g/L}$ – Control.

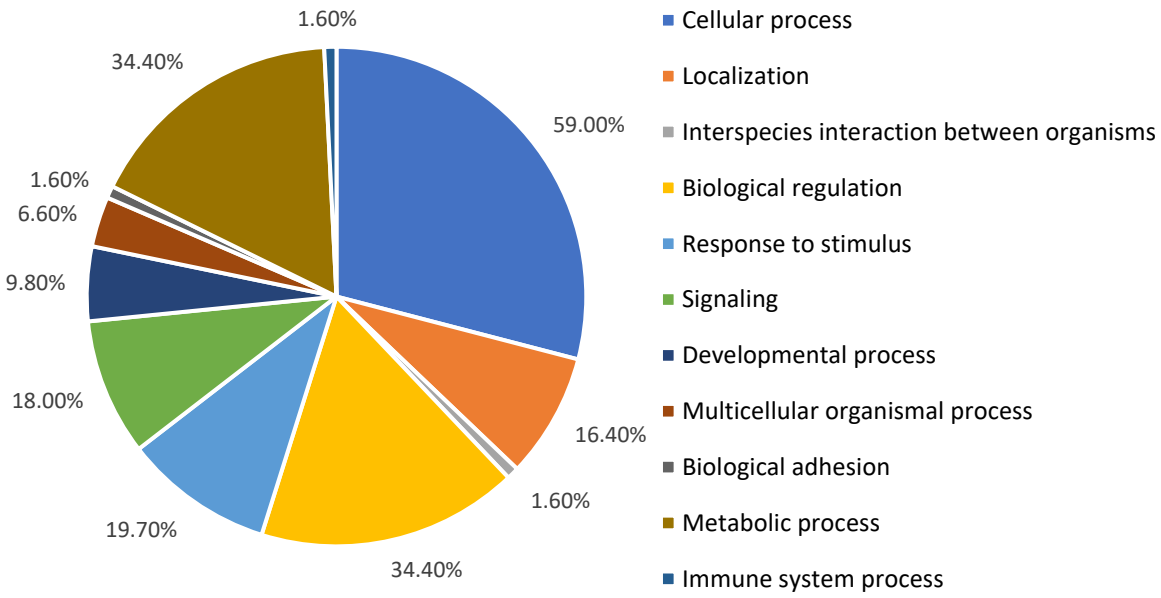

Figure 3.11. A Venn diagram breaking down the biological pathways from Gene Ontology associated with all 66 significantly different gene symbols from the inorganic chromium assay.

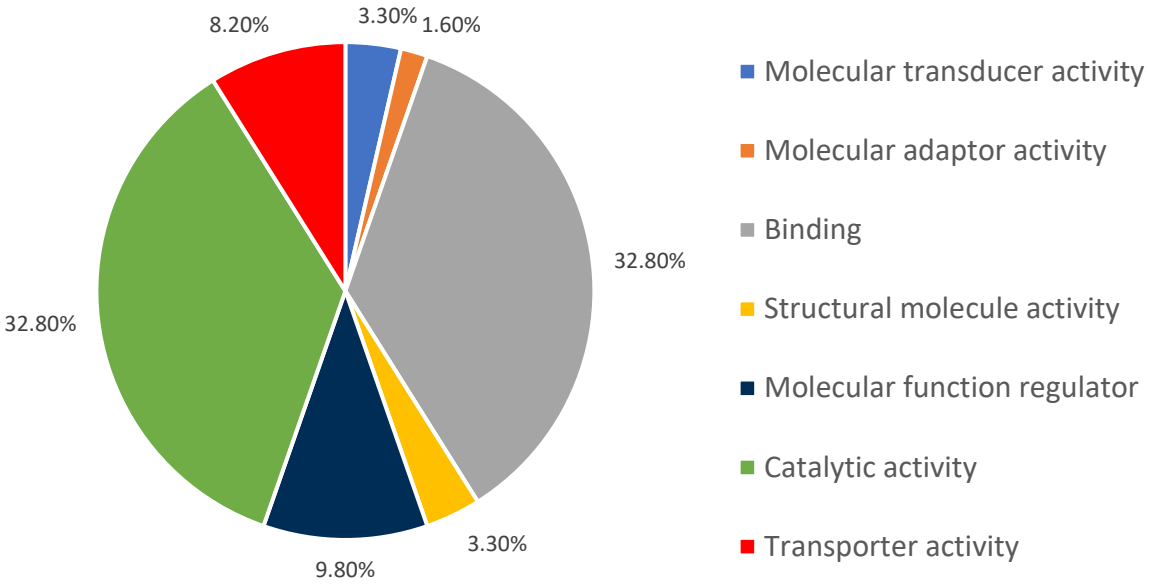

Figure 3.12. A Venn diagram breaking down the molecular functions from Gene Ontology, associated with all 66 significantly different gene symbols from the inorganic chromium assay.

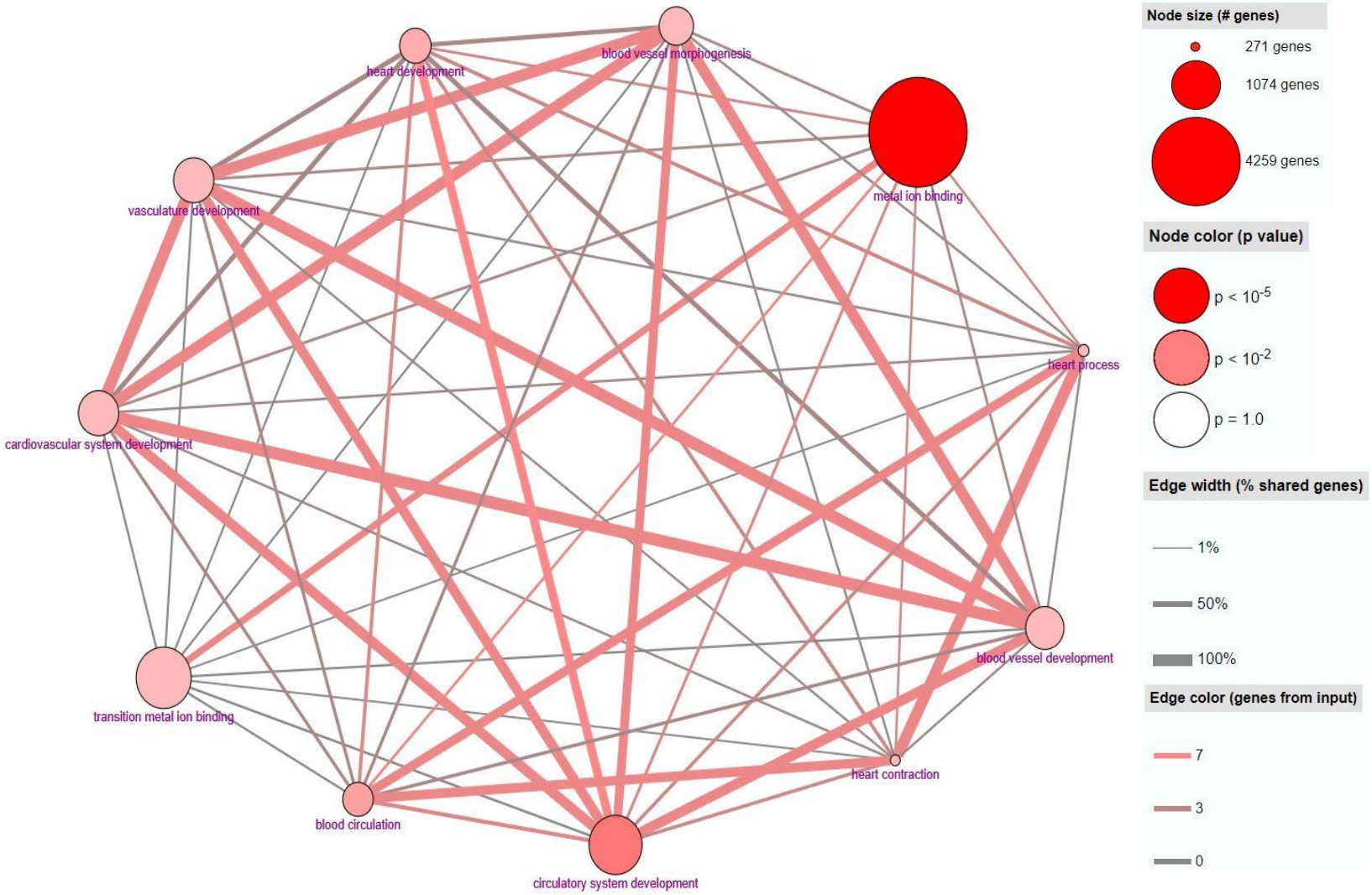

Figure 3.13. A map of the heart related pathways associated with Trim21, Rock2, Jak2, Slc8a1 and Flt1 from Consensus Path Database.

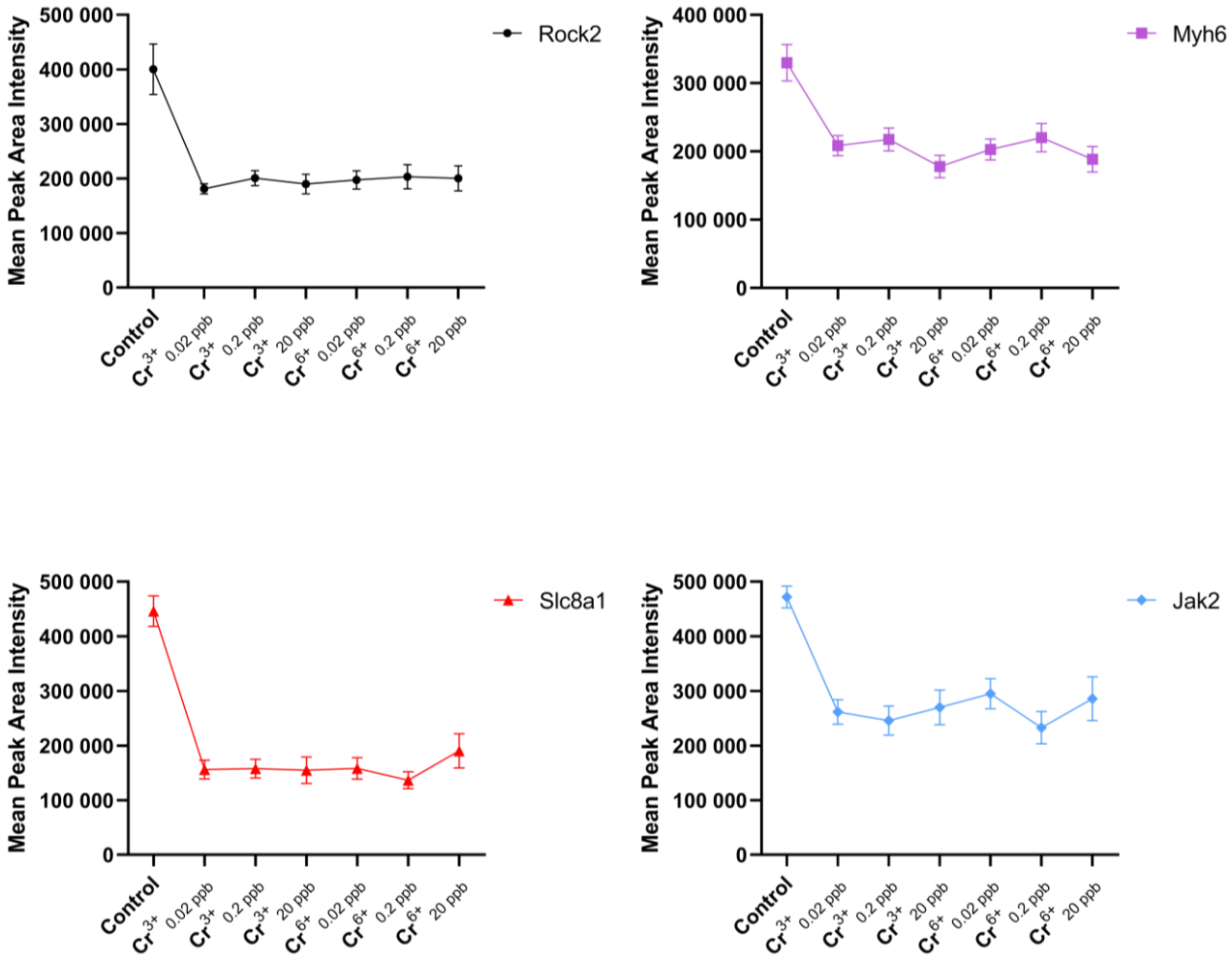

Figure 3.14.1. Dose response curves for the proteins of interest (Rock2, Myh6, Slc8a1, Jak2) that decreased in abundance (from the ANOVA, $p < 0.05$) across the inorganic chromium assay. Each point is the mean of peak areas, and the error bars represent standard error.

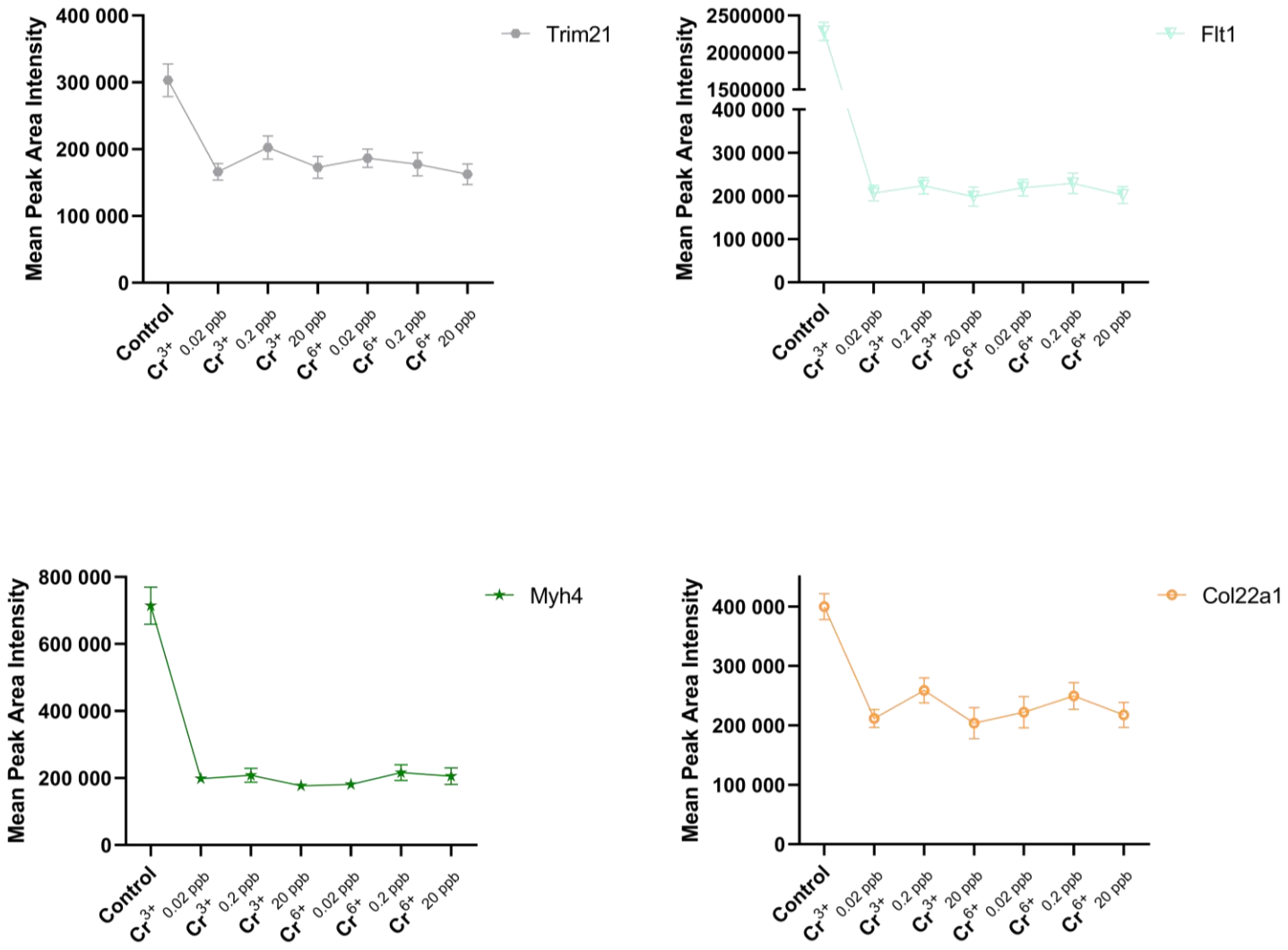

Figure 3.14.2. Dose response curves for the proteins of interest (Trim21, Flt1, Myh4, Col22a1) that decreased in abundance (from the ANOVA, $p < 0.05$) across the inorganic chromium assay. Each point is the mean of peak areas, and the error bars represent standard error.

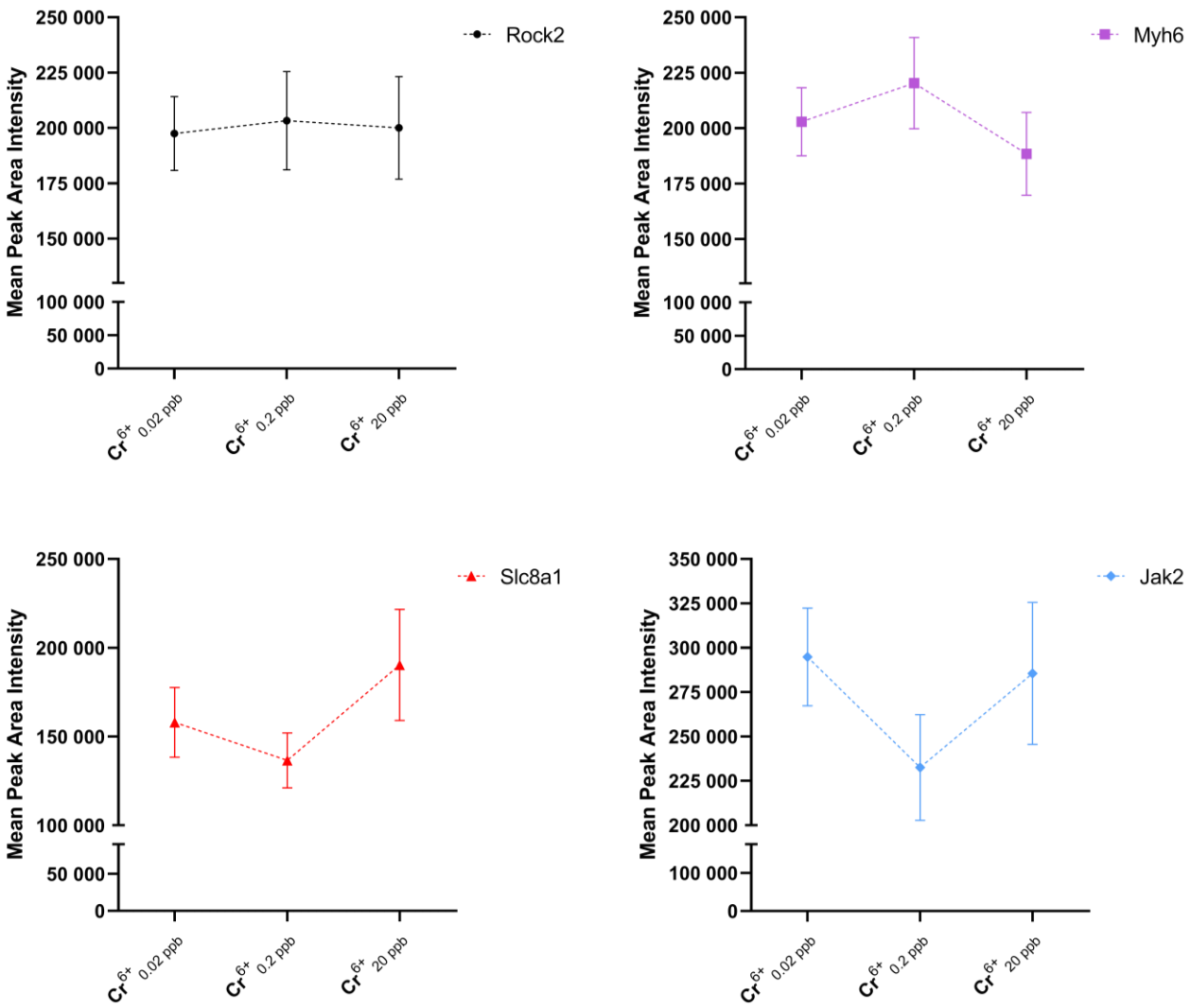

Figure 3.15.1. Dose response curves for the proteins of interest (Rock2, Myh6, Slc8a1, Jak2) that decreased in abundance (from the ANOVA, $p < 0.05$) across the inorganic chromium assay. Each point is the mean of peak areas, and the error bars represent standard error.

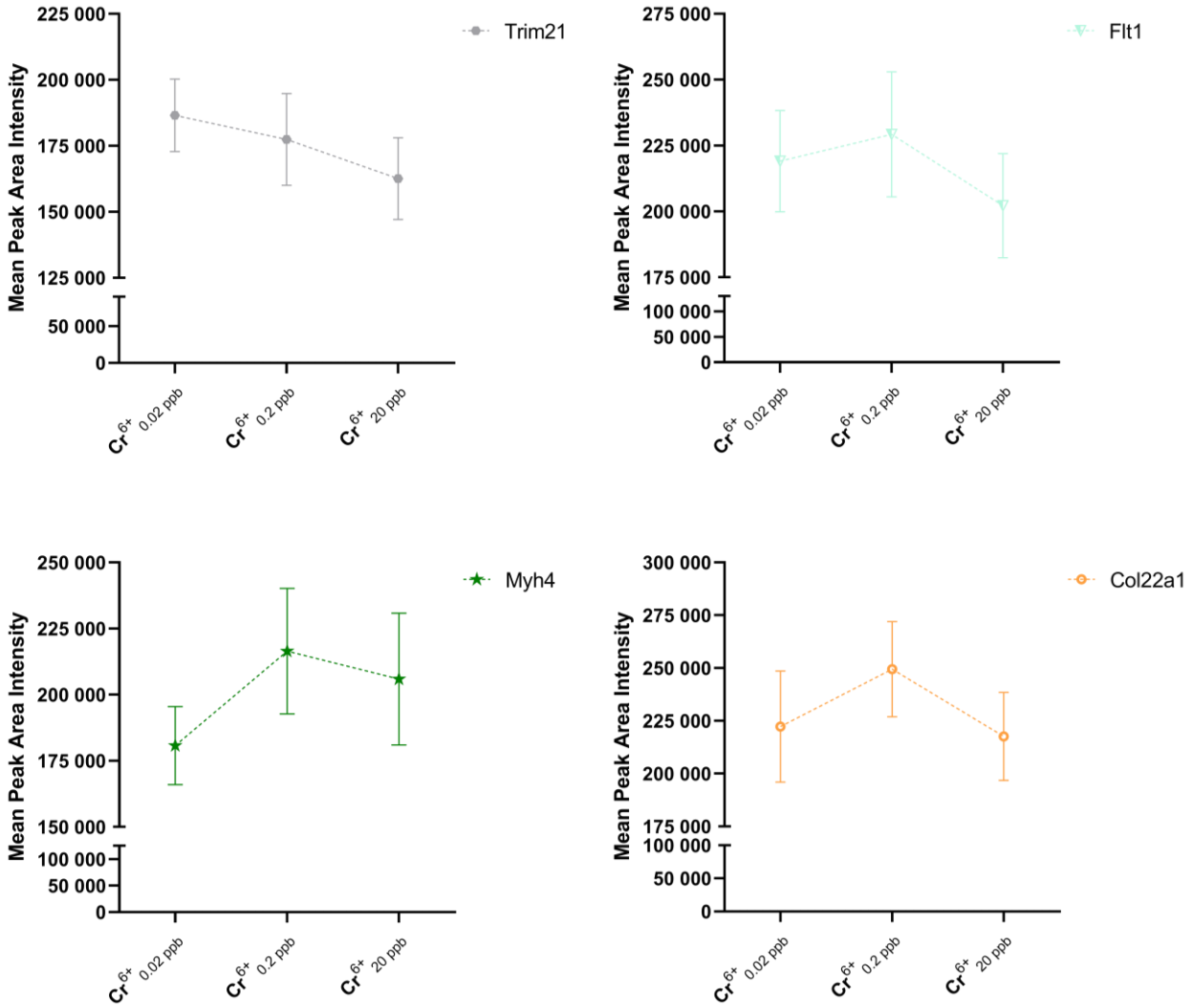

Figure 3.15.2. Dose response curves for the proteins of interest (Trim21, Flt1, Myh4, Col22a1) that decreased in abundance (from the ANOVA, $p < 0.05$) across the inorganic chromium assay. Each point is the mean of peak areas, and the error bars represent standard error.

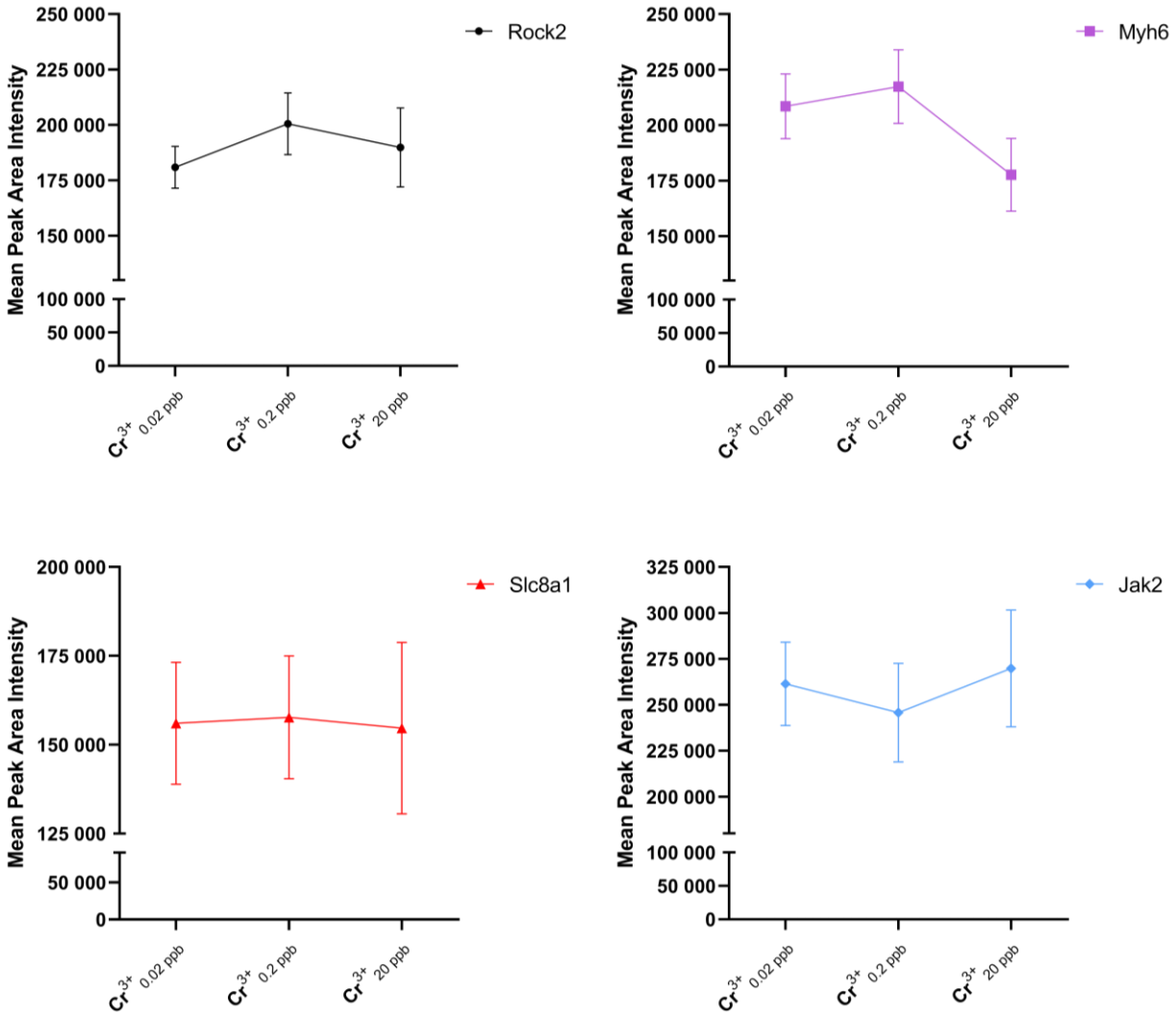

Figure 3.16.1. Dose response curves for the proteins of interest (Rock2, Myh6, Slc8a1, Jak2) that decreased in abundance (from the ANOVA, $p < 0.05$) across the inorganic chromium assay. Each point is the mean of peak areas, and the error bars represent standard error.

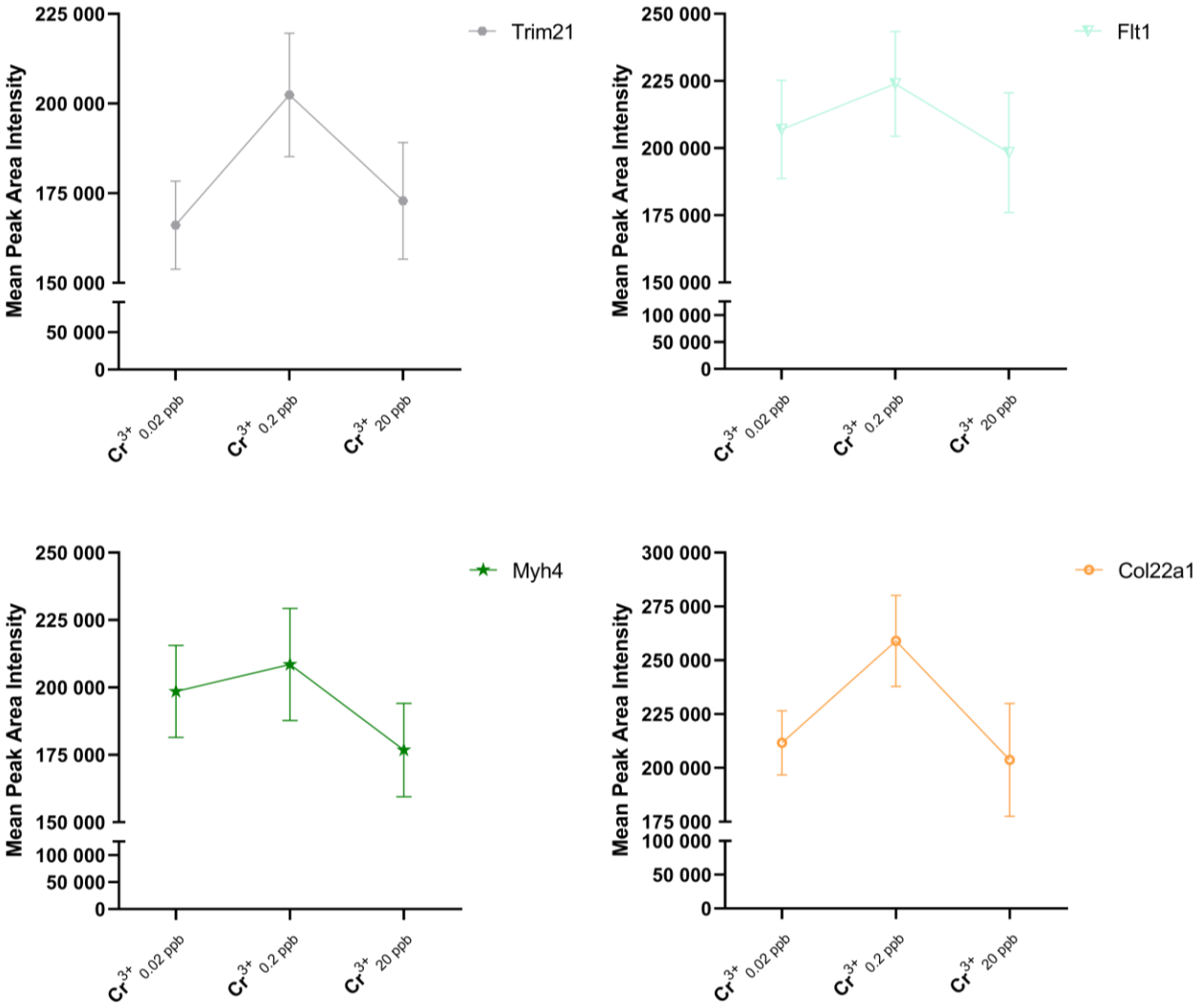

Figure 3.16.2. Dose response curves for the proteins of interest (Trim21, Flt1, Myh4, Col22a1) that decreased in abundance (from the ANOVA, $p < 0.05$) across the inorganic chromium assay. Each point is the mean of peak areas, and the error bars represent standard error.

Table 3.1. Descriptive statistics for the HSI's of rainbow trout exposed to different concentrations of Cr^{3+} and Cr^{6+} (Inorganic Chromium Assay)

	Exposure						
	Control	$Cr^{3+}_{0.02}$ µg/L	$Cr^{3+}_{0.2}$ µg/L	Cr^{3+}_{20} µg/L	$Cr^{6+}_{0.02}$ µg/L	$Cr^{6+}_{0.2}$ µg/L	Cr^{3+}_{20} µg/L
Mean	0.9374	0.9088	1.020	0.9605	1.001	0.9470	1.020
Standard Deviation	0.1200	0.1168	0.2357	0.1595	0.1274	0.1409	0.1710

*n = 20 for all exposure groups.

Table 3.2. Descriptive statistics for the HSI's of rainbow trout exposed to chromium picolinate and metformin HCl (Nutritional Supplement Assay)

	Exposure		
	Control	Chromium Picolinate (20 µg/L)	Metformin HCl (20 µg/L)
Mean	0.9696	0.8875	0.9988
Standard Deviation	0.09906	0.1119	0.1678

*n = 20 for all exposure groups.

Table 3.3. Descriptive statistics for the BGC's of rainbow trout exposed to chromium picolinate and metformin HCl (Nutritional Supplement Assay)

	Exposure		
	Control	Chromium Picolinate (20 µg/L)	Metformin HCl (20 µg/L)
Mean	6.250	5.753	5.120
Standard Deviation	0.9484	0.8596	1.006

*n = 20 for all exposure groups.

Table 3.4. Proteins of interest associated with metal ion binding, from rainbow trout exposed to a range of Cr^{3+} and Cr^{6+} (Inorganic Chromium Assay).

Gene Symbol	*Full Name*	*Description*
Trim21	Tripartite Motif Containing 21	• Trim proteins play roles in cellular processes such as intracellular signaling, innate immunity, transcription, autophagy, and carcinogenesis (55) • Downregulation facilitates hepatocellular carcinoma (56)
Rock2	Rho Associated Coiled-Coil Containing Protein Kinase 2	• Mediate various important cellular functions such as cell shape, motility, secretion, proliferation, and gene expression (57) • Downregulation associated with a decreased risk of dextrocardia and axonal degeneration/apoptosis and cardiovascular benefits (58)
Jak2	Janus Kinase 2	• JAK2 plays a central role in cytokine and growth factor signaling. • Downregulation or mutation is associated with a decreased risk of several myeloproliferative diseases and cancers. • Diagnostic marker that is tested upon myeloproliferative disorder diagnosis (59)
Slc8a1	Solute Carrier Family 8 Member A1	• Plays an important role in Na^{+}-Ca^{2+} ion exchange in the heart (60) • Abundant in cardiac myocytes (61)
Flt1	FMS Related Receptor Tyrosine Kinase 1	• Encodes a member of the vascular endothelial growth factor receptor (VEGFR) family. • Involved in the control of cell proliferation and differentiation. • Plays a role in angiogenesis through VEGF binding (62)

Table 3.5. Proteins of interest associated with circulatory system related pathways, from rainbow trout exposed to a range of Cr^{3+} and Cr^{6+} (Inorganic Chromium Assay).

Gene Symbol	*Full Name*	*Description*
Myh4	Myosin Heavy Chain 4	• Protein coding gene • Downregulation associated with cardiomyopathy • Diseases associated with MYH4 include altered arterial contractility cardiomyopathy (63, 64)
Myh6	Myosin Heavy Chain 6	• Encodes the alpha heavy chain subunit of cardiac myosin • Downregulation associated with systolic disfunction and heart failure. • Diseases associated with MYH6 include Atrial Septal Defect 3 and cardiomyopathy (64)
Col22a1	Collagen Type XXII Alpha 1 Chain	• This gene encodes a member of the collagen family which is thought to contribute to the stabilization of myotendinous junctions and strengthen skeletal muscle attachments during contractile activity • The encoded protein is deposited in the basement membrane zone of the myotendinous junction which is present only at the tissue junctions of muscles, tendons, the heart, articular cartilage, and skin • A knockdown of the orthologous zebrafish gene induces a muscular dystrophy by disruption of the myotendinous junction • Diseases associated with COL22A1 include Diffuse Cutaneous Systemic Sclerosis and Muscular Dystrophy (65)

Chapter 4. Discussion

4.1 Inorganic Chromium Assay

4.1.1 Hepatosomatic Index

No significant differences were identified for HSI, between the control and treatment groups for the inorganic chromium assay. This indicates that there was no change in the energy reserves of the fish due to chromium exposure at the measured concentrations. Therefore, at the concentrations in our assay, the chromium exposure was not a significant enough stressor for the fish to disrupt metabolic function or feeding behaviour. This also indicates that heavy metal-induced fatty liver likely did not develop within the 28-day exposure period. Analysis of the liver tissue would be required to confirm this. It is possible that at higher concentrations, we would have observed an effect on HSI, as has been observed in previous studies (66, 67). The study performed by Shaw et al., had an exposure concentration of 2 mg/L, which is much greater than what was used in our study. They observed major changes to liver tissue structure and lipid peroxidation. The study by Farag et al., used exposure concentrations in parts per billion and is therefore, much more comparable to our study. Their exposure concentrations ranged from 24 to 266 µg/L, and observed lipid droplets in hepatocytes after 105 days exposed to chromium, compared to their control groups that had none (67). Our exposure period was shorter and concentrations lower, thus our result of no significant changes in the HSI of the rainbow trout is not unexpected.

4.1.2 Micronucleus Assay

Significant differences were identified between control and $Cr^{3+}_{0.02\ \mu g/L}$, as well as between control and $Cr^{6+}_{0.2\ \mu g/L}$. This shows that there was an increased rate of split and notched RBC nuclei observed for both treatment groups. However, no other differences were observed. One possible explanation for the changes observed at the lower, but not the higher concentrations of chromium

could be that the repair mechanisms had already been activated at higher doses. However, given that there was no dose-response or trend in chromium species observed, it seems unlikely that the significant changes in RBC nuclei were caused by chromium exposure. Another possibility is that the percentage of abnormal cells are within a normal range of variance. Other studies that have used a micronucleus assay to observe the effects of chromium exposure in fish have much higher rates of abnormal nuclei. The negative control groups in these studies observed abnormality percentages that ranged from 0.1 – 0.32% (68, 69). All of the treatment groups from our study fall into this baseline range. Again, a higher concentration, or longer exposure may have increased the numbers outside of this range, however, based on the results, our exposure concentrations were too low to have a significant effect on the rainbow trout red blood cells.

4.1.3 Protein – Exposure Group Comparison

All three of the Cr^{6+} treatment groups shared many (61/64) of the significantly different proteins identified. All of these proteins were decreased in abundance in comparison to control. This shows that the response to chromium by the fish was nearly identical for the concentration gradient used. A similar result was observed for the three Cr^{3+} treatment groups (56/64 proteins shared), the response to chromium exposure was comparable across all three measured concentrations. This significant overlap of proteins at each exposure concentration also carried over to comparisons made between the two chromium species. The $Cr^{6+}_{0.02\ \mu g/L}$ and $Cr^{3+}_{0.02\ \mu g/L}$ treatment groups shared 62/63 significantly different proteins. $Cr^{6+}_{0.2\ \mu g/L}$ and $Cr^{3+}_{0.2\ \mu g/L}$ treatment groups shared 55/65 significantly different proteins. $Cr^{6+}_{20\ \mu g/L}$ and $Cr^{3+}_{20\ \mu g/L}$ treatment groups shared 62/64 significantly different proteins. All three of these comparisons suggest that there is no difference in the response of Cr^{6+} and Cr^{3+}, at the environmentally relevant concentrations used.

4.1.4 CPDB Pathway Analysis

Using consensus path database (CPDB), we found that within the group of proteins that were significantly decreased in abundance in all exposures compared to control, Trim21, Rock2, Jak2, Slc8a1 and Flt1 are all known to be involved with metal ion binding and circulatory system related pathways. As well, we observed decreased Myh4, Myh6 and Col22a1, which are also proteins involved with circulatory system related pathways.

Dysregulation of the gene that codes for Trim21 is associated with different cancers, immunological diseases, and developmental disorders (55, 70). There is also evidence that shows that tripartite motif (TRIM) family proteins play a role in the regulation of ubiquitin-mediated degradation of oncogene products and tumour suppression (70). Trim21 will be the focus of discussion as it was the only protein in the family that was decreased in abundance and is associated with transition metal ion binding. Reduced expression of Trim21 specifically has been shown to be indicative of poor prognosis in cancer patients and facilitates hepatocellular carcinoma carcinogenesis (HCC) (56). Therefore, based on the decreased Trim21 abundance observed in the blood plasma, it is possible that the rainbow trout exposed to these low levels of chromium for four weeks could possibly be in the early stages of liver disease. Further analysis on our rainbow trout liver samples would help to confirm this notion. Chromium can lead to the development of hepatocytes and necrosis, however, studies where this was observed in fish use 96-hour LC_{50} (can range from 10 mg/L to 40 mg/L depending on the species) as an exposure concentration (68, 71). Studies that use concentrations around 2 mg/L observe lipid peroxidation, chromium accumulation and development of microscopic lesions (66-68). Exposure concentrations even lower in the range of µg/L result in lesser outcomes, such as increased liver mass, altered gene expression or lipid accumulation in hepatocytes (67). Our exposure concentrations were on the extreme low end, and therefore a minimal response in the trout is expected.

Slc8a1 is a protein from a family of genes that encodes Na^{+}/Ca^{2+} exchangers (60, 61). Dysregulation of these genes are associated with heart failure, arrhythmia and hypertension (60). Based on data from the Human Protein Atlas (HPA), Slc8a1 is heavily expressed in heart tissue (72). This makes sense as Ca^{2+} binding within cells is the initiating event in heart muscle contraction (61, 73). Reduced abundance of this protein may suggest that some sort of heart disorder, or disruption of Na^{+}/Ca^{2+} ion exchange within the heart, was developing in the rainbow trout after four weeks of exposure to chromium.

Myosin heavy chains are a class of proteins that are expressed in different muscle tissues (74). These proteins work in tandem with actin to produce chemo-mechanical force (75). A decrease in the abundance of both Myh4 and Myh6 was observed in the rainbow trout plasma of all treatment groups. Within the body, this class of proteins is normally expressed in muscle tissues like skeletal muscle and arteries (63). Myh4 and Myh6 specifically are expressed in medium and high abundance, respectively, in the heart (HPA) (72). Defective myosin heavy chain expression is associated with cardiovascular disorders, such as altered arterial contractility and cardiomyopathy (63, 64). A decrease in abundance of Myh6 specifically is correlated with systolic dysfunction and cardiomyopathy (64). Therefore, the decrease that was observed in the rainbow trout due to chromium exposure may be indicative of the development of cardiomyopathy. There are some studies that show there a cardiotoxic potential from chromium exposure, however, the studies are limited, and none were found that relate to fish (76, 77). We cannot confirm cardiomyopathy development with the assays we performed and tissues we collected; however, future research could explore this possibility.

All of the other proteins detected (Rock2, Jak2, Flt1, Col22a1) either have effects that are too far upstream to correlate with specific adverse outcomes or have minor positive effects that would

counteract the more severe carcinogenic and DNA damaging effects associated with chromium exposure. Decreased abundance of Rock2 is associated with a decreased risk of dextrocardia and axonal degeneration (58). Dextrocardia is a developmental disorder, and our assays were not designed to measure axonal degeneration. Decreased abundance of Jak2 yields a decreased risk of several myeloproliferative diseases and cancers (59). This is a positive that does not outweigh the negatives associated with chromium exposure. Decreased Flt1 abundance may improve angiogenesis by reduced binding activity with vascular endothelial growth factor receptor (VEGF) (62). Again, this is a positive that could be countered by the negatives of chromium exposure. Knocking out the gene that codes for Col22a1 has been shown to induce muscular dystrophy in zebra fish (65). Our assay was not designed to test for this type of higher-level effect. A complete knockout of the gene is required, and we only observed a decreased abundance of protein and therefore a more specific assay design would be required.

4.1.5 Chromium Toxicity

The same handful of adverse effects associated with chromium exposure regarding fish are found throughout the literature. The effects being DNA damage, cytotoxicity and accumulation in gills, liver, skin and muscle. The majority of these effects were observed at extremely high concentrations that would not necessarily be environmentally relevant. Studies often utilize acute toxicity tests using the 96-hour LC_{50} (~120 ppm) as the basis for the exposure concentrations (78, 79). The lowest concentrations in these studies are often much higher that the highest concentration we used in this study. For example, the lowest concentration used by Castro & Moraes was 100 ppm, compared to the 20 µg/L nominal concentration used in our study. High concentration studies are very valuable as it is important to understand the true worst-case scenario exposure to these metals. However, these concentrations are only environmentally relevant in an extreme case of

negligence. Therefore, it is unreasonable to expect to observe the same worst-case scenario adverse effects. Castro & Moraes observed reversible lesions and edema in the skin, vacuolization and hypertrophy of the liver and cell degeneration and focal necrosis in the kidney due to hexavalent and trivalent chromium exposure (78). Their highest treatments even resulted in mortalities. It is notable that in our study, at a concentration 5000x lower, analysis of blood plasma was able to detect a decrease in Trim21 abundance, indicating the potential onset of hepatocellular disease. If our study was extended over a longer period, other similar effects to that of Castro & Moraes, such as the skin or liver disease, may have been detected. Moreover, because we kept our concentrations environmentally relevant to the Ring of Fire region, the carcinogenic potential of the chromium species was not fully reached and toxicity to the fish was low. Recovery to baseline protein abundance levels may even be possible with a depuration period post exposure.

Farag et al. based their concentrations on the groundwater upwellings of the Columbia River in the northwestern United States (67). This makes for an excellent study for comparison to ours as their concentrations are in the µg/L range, and they also used a flowthrough system to expose Chinook salmon to hexavalent chromium. The lowest concentration from Farag et al is 24 µg/L, again, greater than our highest concentration. They observed lesions in, and necrosis of the cells lining kidney tubules, as well as an increase in lipid peroxidation (67). Nuclear DNA damage was also detected (67). In comparison to our study, only their lowest concentration is comparable. Their exposure concentrations range from approximately 2x – 10x those used in our study. We also detected alteration of the blood cell nuclei, as previously mentioned, but not to an extent where we can definitively say that chromium exposure resulted in DNA damage (only in two of six treatments). If our measured exposure concentrations were closer to nominal, then maybe the results would have aligned better. Again, either a higher concentration or an extended exposure

period may have yielded more robust results. Lastly, it is also worth mentioning that kidney tissue necrosis has been observed as an adverse outcome of lower levels of chromium exposure in more than one study (67, 68, 78). The kidney should definitely be a target organ of analysis in future low-dose chromium exposure studies.

4.2 Nutritional Supplement Assay

As previously mentioned, 4018 proteins were detected in this assay and none of them were significantly different from the control. In some ways this makes sense because the concentration of chromium picolinate and metformin were very low. Previous metformin studies in our lab found that there were no significant effects on adult Japanese Medaka exposed to metformin concentrations ranging from 1 µg/L to 100 µg/L (80). The rainbow trout in our study are much larger, older and therefore likely more resilient to effects of low concentration metformin exposure. The chromium picolinate concentration was even lower, as the total chromium was below the MDL for our water test. This was likely due to the poor solubility of chromium picolinate, which may also result in poor bioavailability in the fish. We used DMSO as a carrier solvent to try and increase chromium picolinate's solubility, but what did not precipitate out of the water may still have been poorly absorbed by the fish. Further study would be needed to say this for sure. Moreover, the blood glucose concentration analysis only resulted in one significant difference between control and metformin. This shows that metformin was a successful positive control and did have an insulin sensitizing effect in the fish. However, even though a significant difference was detected in blood glucose concentration, no difference was detected in the blood plasma for this assay. This may be an effect that is better detected in the liver, and we believe this is reason to analyze our liver samples in future studies. Chromium picolinate concentration had no influence on blood glucose levels, again, likely due to the concentration being too low.

4.3 Conclusion

At concentrations relevant to the Ring of Fire region of Northern Ontario, hexavalent and trivalent chromium had no significant effect on hepatosomatic index during our inorganic chromium assay. All concentrations of the individual chromium species shared the same approximately 60 proteins that decreased in abundance. When comparing the proteins that changed from hexavalent and trivalent chromium exposure individually, again, the same 60 proteins differed in comparison to control. No notable differences were observed between hexavalent and trivalent chromium exposure, and a decrease in Trim21, Slc8a1, Myh4 and Myh6 was observed in all treatments. Reduced abundance of Trim21 is associated with hepatocellular carcinoma, and Slc8a1, Myh4 and Myh6 are all associated with cardiomyopathy. However, we cannot say for sure that the fish had these ailments as analysis of those organs would be required. Future chromium exposure studies on fish should increase focus on the liver, kidney, and the heart. The kidney was a missed opportunity for this study as necrosed tissue seems to be a reoccurring theme within the literature, and the heart was an unexpected organ of interest. Overall, both hexavalent and trivalent chromium exhibit similar effects at low doses in relation to plasma protein abundances in fish and therefore measuring total chromium for environmental monitoring should be sufficient at low concentrations. Future environmental monitoring programs in the Ring of Fire region, especially near the smelter, could potentially use the 0.02 µg/L – 20 µg/L concentration range as a protective gradient to maintain the health of larger aquatic vertebrates like rainbow trout.

For our nutritional supplement assay, chromium picolinate had no effect on blood glucose concentration compared to metformin, which was successful at sensitizing the insulin response in the fish, and lowering a food induced blood glucose spike. Both chromium picolinate and metformin had no measurable effect on the protein abundance of blood plasma. Chromium

picolinate has very low solubility in water and that likely played a factor in the minimal effect on the rainbow trout.

Appendices

Appendix A.

A1. Chromium Mass Spectrometer Methods

Acquisition Method Report

Agilent | Trusted Answers

Acquisition Method Info

Method Name	Agilent_training_peptides_slope4.m
Method Path	D:\MassHunter\Methods\peptides\Agilent_training_peptides_slope4.m
Method Description	

Device List

- Multisampler
- Binary Pump
- Column Comp.
- Q-TOF

TOF/Q-TOF Mass Spectrometer

Component Name	MS Q-TOF	**Component Model**	G6545A
Ion Source	Dual AJS ESI	**Stop Time (min)**	No Limit/As Pump
Can wait for temp.	Enable	**Fast Polarity**	False
MS Abs. threshold	500	**MS Rel. threshold(%)**	0.010
MS/MS Abs. threshold	5	**MS/MS Rel. threshold(%)**	0.010

Time Segments

Time Segment #	Start Time (min)	Diverter Valve State	Storage Mode	Ion Mode
1	0	MS	Both	Dual AJS ESI

Time Segment 1

Acquisition Mode AutoMS2

MS Min Range (m/z)	200
MS Max Range (m/z)	3000
MS Scan Rate (spectra/sec)	3.00
MS/MS Min Range (m/z)	50
MS/MS Max Range (m/z)	3000
MS/MS Scan Rate (spectra/sec)	2.00
Isolation Width MS/MS	Medium (~4 amu)
Decision Engine	Native

Ramped Collision Energy

Charge	Slope	Offset
All	4	2

Auto MS/MS Preferred/Exclude Table

Mass	Delta Mass (ppm)	Charge	Type	Retention Time (min)	Delta Ret. Time (min)	Isolation Width	Collision Energy
921.9686	100	1	Exclude	0		Narrow (~1.3 amu)	

Precursor Selection

Max Precursors Per Cycle	10
Threshold (Abs)	500
Threshold (Rel)(%)	0.010
Precursor abundance based scan speed	Yes
Target (counts/spectrum)	25000.000
Use MS/MS accumulation time limit	Yes
Use dynamic precursor rejection	No
Purity Stringency (%)	100.000
Purity Cutoff (%)	30.000
Isotope Model	Peptides
Active exclusion enabled	Yes
Active exclusion excluded after (spectra)	2
Active exclusion released after (min)	0.20
Sort precursors	By abundance only

Static Exclusion Ranges

StartMZ	EndMZ
25	300

Charge State Preference

Selected Charges
2
3
>3

Instrument Parameters

Parameter	Value
Gas Temp (°C)	325
Gas Flow (l/min)	8
Nebulizer (psig)	35
SheathGasTemp	350
SheathGasFlow	11

Scan Segments

Scan Seg #	Ion Polarity
1	Positive

Scan Segment 1

Scan Source Parameters

Parameter	Value
VCap	4500
Nozzle Voltage (V)	1000
Fragmentor	180
Skimmer1	65
OctopoleRFPeak	750

ReferenceMasses

Ref Mass Enabled	Disabled
Ref Nebulizer (psig)	

Chromatograms

Chrom Type	Label	Offset	Y-Range
TIC	TIC	15	10000000
TIC	TIC	15	10000000

Name: Multisampler **Module: G7167A**

Sampling Speed	
Draw Speed	100.0 µL/min
Eject Speed	400.0 µL/min
Wait Time After Drawing	1.2 s
Injection	
Needle Wash Mode	Standard Wash
Injection Volume	2.00 µL
Standard Needle Wash	
Needle Wash Mode	Flush Port
Duration	10 s
High Throughput	
Injection Valve to Bypass for Delay Volume Reduction	No
Sample Flush-Out Factor	5.0
Overlapped Injection	
Overlap Injection Enabled	No
Needle Height Position	
Draw Position Offset	-1.0 mm
Use Vial/Well Bottom Sensing	No
Stop Time	
Stoptime Mode	No Limit
Post Time	
Posttime Mode	Off

Name: Binary Pump **Module: G7112B**

Flow	0.000 mL/min
Use Solvent Types	Yes
Low Pressure Limit	0.00 bar
High Pressure Limit	400.00 bar
Maximum Flow Gradient	100.000 mL/min²
Stroke A	
Automatic Stroke Calculation A	Yes
Stroke B	
Automatic Stroke Calculation B	Yes
Stop Time	
Stoptime Mode	Time set
Stoptime	50.00 min
Post Time	
Posttime Mode	Off

Solvent Composition

	Channel	Solvent 1	Name 1	Solvent 2	Name 2	Selected	Used	Percent (%)
1	A	H20		H20		Ch. 1	Yes	98.0 %
2	B	premixed ACN(95%) - H2O(5%)		ACN		Ch. 1	Yes	2.0 %

Timetable

	Time (min)	A (%)	B (%)	Flow (mL/min)
1	0.00 min	98.0 %	2.0 %	0.100 mL/min
2	2.00 min	98.0 %	2.0 %	0.100 mL/min

	Time (min)	A (%)	B (%)	Flow (mL/min)
3	27.00 min	60.0 %	40.0 %	0.100 mL/min
4	32.00 min	40.0 %	60.0 %	0.100 mL/min
5	32.01 min	15.0 %	85.0 %	0.100 mL/min
6	37.00 min	15.0 %	85.0 %	0.100 mL/min
7	37.01 min	98.0 %	2.0 %	0.100 mL/min

Name: Column Comp.	Module: G7116A
Left Temperature Control	
Temperature Control Mode	Temperature Set
Temperature	40.0 °C
Enable Analysis Left Temperature	
Enable Analysis Left Temperature On	Yes
Enable Analysis Left Temperature Value	1.0 °C
Left Temp. Equilibration Time	0.0 min
Right Temperature Control	
Right temperature Control Mode	Temperature Set
Right temperature	40.0 °C
Enable Analysis Right Temperature	
Enable Analysis Right Temperature On	Yes
Enable Analysis Right Temperature Value	0.8 °C
Right Temp. Equilibration Time	0.0 min
Enforce column for run	
Enforce column for run enabled	No
Stop Time	
Stoptime Mode	As pump/injector
Post Time	
Posttime Mode	Off
Timetable	
Valve Position	Position 2 (Port 1 -> 2)
Position Switch After Run	Do not switch

Plasma protein digestion

Samples were thawed on ice, and immediately upon complete thaw, we transferred 15 µL of plasma to a low retention microcentrifuge tube with 35 µL of 100 mM Ammonium Bicarbonate (AB) Buffer and mixed with gentle vortex. We then reduced the proteins in the plasma with the addition of 2.65 µL of 100 mM of tris(2-carboxyethyl)phosphine in 100 mM AB buffer, mixed using gentle vortex, and allowed to incubate at room temperature for 45 min. Proteins were then alkylated with the addition of 2.8 µL of 200 mM iodoacetamide in 100 mM AB buffer, vortexed gently, and incubated in the dark at room temperature for 45 min. At the end of the second incubation, 50 µL of chemical digestion solution (20% formic acid v/v) was added to each sample and vortexed for 5 s. Lid locks were placed on each tube and incubated at 115 ◦C for 30 min in a heating block (VWR 96 place heating block). Samples were dried in a centrifugal evaporator (SpeedVac, Thermo-Fisher) for 40 min. Dried samples were stored at 4 ◦C overnight, and then resuspended in 20 µL of 95% H2O 5% acetonitrile and 0.1% formic acid. Samples were vortexed until dried pellets were completely dissolved, and then centrifuged for 10 min at 14000 ×g. 20 µL of the sample supernatant and 1 µL of internal peptide standard (H2016, Sigma-Aldrich, Oakville, ON) were added to 2 mL screw thread HPLC vials (Chromatographic Specialties, 12 × 32 mm) containing 250 µL pp. bottom spring inserts (Canadian Life Sciences, 6 × 29 mm). Samples were stored at 4 ◦C until instrumental analysis.

2 µL of the peptide solution from each sample were injected and then separated by reverse phase liquid chromatography using a Zorbax, 300SB-C18, 1.0 × 50 mm 3.5 µm column (Agilent Technologies Canada Inc., Mississauga, ON) using an Agilent 1260 Infinity Binary LC. The Agilent 6545 Accurate-Mass Quadrupole Time of- Flight (Q-TOF) was used as the detector in tandem to the Agilent 1200 series liquid chromatography system (see detailed instrumental methods are available in Appendix III).

Each analytical run included a solvent blank and a BSA digest standard (Agilent Technologies Canada Inc., Mississauga, ON) injection every 10 samples in order to monitor baseline, carry-over, drift, and sensitivity during the runtime. The plasma samples were injected once per each individual fish.

Spectral files for each sample were analyzed using Spectrum Mill Software (Version B.04.01.141). Peptides were searched against the Uniprot Reference Proteome Peptides were searched against the Uniprot Reference Proteome ID# UP000193380 for *Oncorhynchus mykiss* (Species ID: 8022; 46447 proteins; downloaded February 2021).

Proteins were then manually validated and accepted when at least one peptide had a peptide score (quality of the raw match between the observed spectrum and the theoretical spectrum) greater than 5 and a %SPI (percent of the spectral intensity that are accounted for by theoretical fragments) of greater than 60% (these settings are recommended by the manufacturer for validating results obtained with an Agilent Q-TOF mass spectrometer). After peptides were sequenced and identified by Spectrum Mill at the MS/MS level, quantification at the MS1 level was performed using the DDA workflow in Skyline 20.2 (MacCoss Lab Software) with a score of 0.9, retention time window of 5 mins, and 5 missed cleavages with transition settings for TOF (Pino et al., 2020).

Statistical Analyses

Data were sorted and manually consolidated using Excel. Statistical analysis was performed with Mass Profiler Professional. Missing values were replaced with 1/5 of the limit of detection (LOD), normalized (for proteins using median, pareto scaling), and ANOVA (Fisher's LSD post-hoc test with Benjamini-Hochberg FDR) were conducted with the normalized data.

References

Pino, LK, Searle, BC, Bollinger, JG, Nunn, B, MacLean, B, MacCoss, MJ. The Skyline ecosystem: Informatics for quantitative mass spectrometry proteomics. Mass Spec Rev. 2020; 39: 229 1– 244. https://doi.org/10.1002/mas.21540

A2. Metformin Mass Spectrometer Methods

Acquisition Method Report

Agilent | Trusted Answers

Acquisition Method Info

Method Name metaboHILICpos_msonly_low_pH.m

Method Path D:\MassHunter\Methods\metabolites\HILIC\metaboHILICpos_msonly_low_pH.m

Method Description

Device List

Multisampler
Binary Pump
Column Comp.
Q-TOF

TOF/Q-TOF Mass Spectrometer

Component Name	MS Q-TOF	**Component Model**	G6545A
Ion Source	Dual AJS ESI	**Stop Time (min)**	No Limit/As Pump
Can wait for temp.	Enable	**Fast Polarity**	False
MS Abs. threshold	1000	**MS Rel. threshold(%)**	0.010
MS/MS Abs. threshold	5	**MS/MS Rel. threshold(%)**	0.010

Time Segments

Time Segment #	Start Time (min)	Diverter Valve State	Storage Mode	Ion Mode
1	0	MS	Both	Dual AJS ESI

Time Segment 1

Acquisition Mode MS1

Min Range (m/z)	50
Max Range (m/z)	1000
Scan Rate (spectra/sec)	1.00

Instrument Parameters

Parameter	Value
Gas Temp (°C)	225
Gas Flow (l/min)	6
Nebulizer (psig)	40
SheathGasTemp	225
SheathGasFlow	10

Scan Segments

Scan Seg #	Ion Polarity	Collision Energy
1	Positive	0

Scan Segment 1

Scan Source Parameters

Parameter	Value
VCap	3000
Nozzle Voltage (V)	0
Fragmentor	125
Skimmer1	65
OctopoleRFPeak	450

ReferenceMasses

Ref Mass Enabled	Disabled
Ref Nebulizer (psig)	

Chromatograms

Chrom Type	Label	Offset	Y-Range
TIC	TIC	15	10000000
TIC	TIC	15	10000000

Name: Multisampler **Module: G7167A**

Sampling Speed

Draw Speed	100.0 µL/min
Eject Speed	400.0 µL/min
Wait Time After Drawing	1.2 s

Injection	
Needle Wash Mode	Standard Wash
Injection Volume	5.00 µL
Standard Needle Wash	
Needle Wash Mode	Flush Port
Duration	3 s
High Throughput	
Injection Valve to Bypass for Delay Volume Reduction	No
Sample Flush-Out Factor	5.0
Overlapped Injection	
Overlap Injection Enabled	No
Needle Height Position	
Draw Position Offset	-1.0 mm
Use Vial/Well Bottom Sensing	No
Stop Time	
Stoptime Mode	No Limit
Post Time	
Posttime Mode	Off

Name: Binary Pump **Module: G7112B**

Flow	0.250 mL/min
Use Solvent Types	Yes
Low Pressure Limit	0.00 bar
High Pressure Limit	500.00 bar
Maximum Flow Gradient	100.000 mL/min²
Stroke A	
Automatic Stroke Calculation A	Yes
Stroke B	
Automatic Stroke Calculation B	Yes
Stop Time	
Stoptime Mode	Time set
Stoptime	25.00 min
Post Time	
Posttime Mode	Time set
Posttime	1.00 min

Solvent Composition

	Channel	Solvent 1	Name 1	Solvent 2	Name 2	Selected	Used	Percent (%)
1	A	H20		H20		Ch. 2	Yes	2.0 %
2	B	premixed ACN(95%) - H2O(5%)		premixed ACN(90%) - H20(10%)		Ch. 2	Yes	98.0 %

Timetable

	Time (min)	A (%)	B (%)	Flow (mL/min)
1	0.00 min	2.0 %	98.0 %	0.250 mL/min
2	3.00 min	2.0 %	98.0 %	0.250 mL/min
3	11.00 min	30.0 %	70.0 %	0.250 mL/min
4	12.00 min	40.0 %	60.0 %	0.250 mL/min
5	16.00 min	95.0 %	5.0 %	0.250 mL/min
6	18.00 min	95.0 %	5.0 %	0.250 mL/min
7	19.00 min	2.0 %	98.0 %	0.250 mL/min
8	25.00 min	2.0 %	98.0 %	0.250 mL/min

Name: Column Comp. **Module: G7116A**

Left Temperature Control	
Temperature Control Mode	Not Controlled
Enable Analysis Left Temperature	
Enable Analysis Left Temperature On	Yes

	Pressure (bar)
1	500.00 bar
2	500.00 bar
3	500.00 bar
4	500.00 bar
5	500.00 bar
6	500.00 bar
7	500.00 bar
8	500.00 bar

Enable Analysis Left Temperature Value	0.8 °C
Left Temp. Equilibration Time	0.0 min
Right Temperature Control	
Right temperature Control Mode	Temperature Set
Right temperature	25.0 °C
Enable Analysis Right Temperature	
Enable Analysis Right Temperature On	Yes
Enable Analysis Right Temperature Value	0.8 °C
Right Temp. Equilibration Time	0.0 min
Enforce column for run	
Enforce column for run enabled	No
Stop Time	
Stoptime Mode	As pump/injector
Post Time	
Posttime Mode	Off
Timetable	
Valve Position	Position 1 (Port 1 -> 6)
Position Switch After Run	Do not switch

Appendix B.

B1. Total Chromium Samples

Five samples for total Cr were taken, one from each of the experimental tanks, by adding 25 mL of tank water to a 50 mL falcon tubes. Samples were packed with ice and shipped overnight to the Purdue Central Analytical Facility at Laurentian University (Sudbury, Ontario, Canada). All five tank samples were acidified using trace -grade HNO_3 to a concentration of 1% acid (360 µL in 25 mLs of sample water; 67-70% purity, Fischer Chemicals™) immediately upon arrival. Samples were stored in the refrigerator overnight and analyzed for total Cr (and other elements) the following day on a Perkin Elmer® NexION 1000 inductively coupled plasma mass spectrometer (ICP-MS) under dynamic reaction cell (DRC) and kinetic energy discrimination (KED) detection modes. KED and DRC were used to remove any polyatomic interferences that may have been present; results between the two modes were in good agreement (data not shown)

and DRC results are presented here, at the recommendation of industry professionals. Prior to analyses, the ICP-MS was optimized using the Smart Tune manager in the Syngystics™ software, as per manufacture instructions. All samples were scanned three times and the relative standard deviation (RSD) of readings were monitored. Other quality assurance and control (QAQC) measures included instrument and method blanks, duplicate samples, an intra-lab reference material, spiked samples, and an internal standard (see Table SI-1).

The data from this initial analysis showed low recoveries of the internal standard, which is used to correct for daily biases in detection (percent recoveries ranged from 34.2 to 44.0%; Table SI-1). While this issue was consistent across all samples and calibration standards, likely making the results valid, the samples were covered with parafilm and stored in the refrigerator until re-analysis, approximately 8 weeks later (on April 12, 2021), after a full system optimization. Internal recoveries range from 81.4 to 95.6% during re-analysis. All other QAQC checks were also within accredited standards (±30%; Table SI-1), with the exception of one instrument spike (which was stored with the samples from Feb-April) for an unknown reason; the percent recovery of a second instrument spike run on April 13, 2021, was high (94.5%; Table SI-1). (It is noteworthy that the results from Feb 11th/12th and April 12th were in good agreement with each other. This is likely due to the low internal standard recovery being consistent across all samples and standards, meaning the samples were compared against a calibration curve with the same internal standard correction applied. This adds confidence to the results, in my opinion.) Three samples were also re-analyzed 24-hours after this second analysis, as an additional QAQC check. Overall, results among the 3 analytical runs were in good agreement (see Table SI-1). The method detection limits (MDL) for total Cr was 0.06 ng/mL. No blank corrections were made to any of the results.

B2. Chromium Speciation Samples

To assess the speciation of Cr in the various treatments, samples of tank water were preserved by adding sodium hydroxide (NaOH, to a concentration of 50mM), sodium carbonate (Na2CO3, to a concentration of 28mM), and ethylenediaminetetraacetic acid (EDTA, to a concentration of 10mM). To achieve the desired molarities, 0.05 g of NaOH (Fisher Chemicals A.C.S. Certified, 97.4%), 0.075 g of Na2CO3 (Fisher Chemicals Enzyme Grade, 99%), and 0.05 g of EDTA (Fisher Chemicals Electrophoresis Grade, 99%) were added to 25mL of tank water in 50 mL falcon tubes. The resulting samples had an elevated pH (>11), which stabilized any Cr(VI) present and prevented it from reducing into Cr(III). Simultaneously, the added EDTA readily complexed with the Cr(III), stabilizing it and preventing oxidation into Cr(VI). Together, these effects helped to limit interconversion between Cr(III) and Cr(VI) after sampling and before analysis. After the reagent additions, samples were gently inverted 5-10 times and heated using a Cole-Parmer sonicator at 60˚C for 60 minutes to speed-up the EDTA-Cr(III) complexation. Samples were cooled to room temperature, packed in with ice packs, and shipped overnight for analysis.

This preservation method was based on EPA Method 3060A and observed stability of method blanks (i.e. ultra-pure water) during digestion trials (data not shown). Before applying the method to samples, two stability trials were run over a 5- and 7- day period (for a full description of the trials and results see Table SI-2, SI-3, and Figure SI-1): recoveries were acceptable (86.5-113.8%) for both Cr(III) and Cr(VI) when they were spiked at a higher-level (20-30 ng/mL, n = 10) across all sampling events, regardless of the heating method applied when the samples were made (i.e., not heated, sonicated, heated on a hot block, or heated on a hot plate). However, the recoveries of spikes at the lower-level (3 ng/mL) were initially high (88.7 to 112.0%), but declined over the 7-day period (to as low as 41.8%; see Table SI-3 for more detail),

potentially suggesting that interconversion had occurred. As such, only tank water from high-level exposures (i.e., 20 ng/mL Cr(III), Cr(VI), and Picolinate) were analyzed for Cr speciation herein.

All preserved samples were analyzed for Cr speciation at the Purdue Central Analytical Facility at Laurentian University within 24-hours of collection. Sample were injected into an Metrohm® 940 Ion Professional IC Vario ion chronography (IC) system, equipped Metrosep Supp4 chromatography column (Metrohm®) to separate Cr(III) from Cr(VI). Species were eluted from the column using a 2mM EDTA eluent (pH raise to 10.1-10.5 using NH4OH) and detected using the Perkin Elmer® NexION 1000 ICP-MS. Detection was performed in DRC mode. All speciation samples were diluted 10-fold prior to analysis to reduce salt loading on the ICP and baseline interferences (Figure SI-3). The MDLs and limits of quantification (LOQs) were estimated to be 0.1±0.03 and 0.3±0.08 for Cr(III), respectively, and 0.1±0.03 and 0.2±0.10 for Cr(VI), respectively. Detected counts per second (CPS) were compared against a linear calibration curve ($R2 > 0.9999$ for both Cr(III) and Cr(VI)). The percentage of deviation from expected concentrations of all calibration standards were between -9.2 to 16.7% across both Cr species. Daily optimization was performed on the ICP-MS using Perkin Elmer's Smart Tune function in the Syngystics™ software as per manufacture instructions; all other operations were performed from Empower3® Chromatography Software from Waters®, which enabled communication between the IC and ICP-MS instruments.

Several QAQC tests were also performed during IC-ICP-MS speciation analysis. First, each tank was sampled and preserved twice and the percentage difference between these method duplicate samples was 12.1% for the 20 ng/mL Cr(III) tank and -1.7% for the 20 ng/mL Cr(VI) tank; no Cr(III) or Cr(VI) was detected in either of the 20 ng/mL picolinate samples. Second, the

20 ng/mL Cr(III) and Cr(VI) samples were retested 5-days after collection and preservation, with the re-tested results being -12.5% and -9.2% different when compared to the initial values. A duplicate injection of the 20 ng/mL Cr(III) tank sample was also performed as an instrument duplicate, and it was 5.6% different from the original value. A second duplicate of this samples was also spiked at 5 ng/mL Cr(III) and Cr(VI), with 97.5% and 96.0% of the Cr recovered for the two species, respectively. Ongoing precision replicates (OPRs), with 1 ng/mL of Cr(III) and Cr(VI), were analyzed in the middle and end of the analytical run; 99.5% and 99.4% of Cr(III) and 102.8% and 104.2% of Cr(VI) was recovered from these two tests. Throughout the analysis, four eluent blanks were also analyzed as instrument blanks, and no Cr(III) or Cr(VI) was detected in any of these samples. Similarly, two method blanks (distilled (DI) water and MilliQ water) were preserved using the same method as samples and analyzed for Cr(III) and Cr(IV) and neither Cr species was detected therein using IC-ICP-MS. Lastly, three tank samples, the 20 ng/mL Cr(III), Cr(VI), and picolinate, and the two blanks samples (DI water and MilliQ water) were analyzed for total Cr by diluting 1 mL of sample in 9mL of 1% HNO_3. ICP-MS analysis was performed following the same methods described in section 1 above and the results were in good agreement with the speciation results (Table 1). It is noteworthy that, despite no detection of Cr(III) or Cr(IV) in speciation analysis, 0.4 to 0.9 ng/mL total Cr was detected in the DI and MilliQ blanks across the three analytical runs. However, no blank subtractions were applied to samples because the speciation of the Cr was unknown.

Table 1 – Chromium speciation and concentrations in the various treatments. Speciation samples were preserved using 10mM EDTA, 50mM NaOH, and 28mM Na2CO3 and were diluted 10X before analysis. HNO_3 was added to acidify samples for total Cr analysis, to a concentration of 1% (v/v), and were directly injected into the ICP for analysis. No Cr(III) nor Cr(VI) was detected in the method blank during speciation analysis, though 0.4-0.9ng/mL of total Cr was detected in these samples during ICP-MS analysis. Note: NA = not analyzed because expected sample concentration was <MDL after 10X dilution; ND = not detected. *indicates that the integration peak was manually adjusted.

	Tank information				*Measured chromium concentrations (ng/mL)*			
Exposure	**Temp (°C)**	**D.O. (mg/L)**	**Cond (µS/cm)**	**pH**	**[Cr(III)]**	**[Cr(VI)]**	**Total [Cr] (speciation)[3]**	**Total [Cr] (acidified)[4]**
Cr(III), 20µg/L	12.7	10	330	8.18	8.44[1]	ND[2]	11.37	11.37
Cr3(III), 0.2µg/L	13	8.7	331	8.09	NA	NA	NA	0.24
CrPic, 20µg/L	12.5	9.5	331	8.15	ND	ND	2.62	1.36
Cr(VI), 20µg/L	12.5	9.4	330	8.17	ND	9.85[5]	8.56	7.83
Cr(VI), 0.2µg/L	12.3	10.2	331	8.15	NA	NA	NA	0.25

[1]Duplicate sample = 7.35* ng/mL; re-analysis three days later = 9.57* ng/mL
[2]A rise in chromatographic baseline was identified as a peak, calculated at 0.156 ng/mL, but it was not considered a true detection; duplicate sample = ND; re-analysis three days later = ND;
[3]Speciation samples were also analyzed for total [Cr] by diluting the preserved sample 10x into 1%HNO_3 before ICP-MS analysis.
[4]Blank concentration = 0.45-0.98 ng/mL
[5]Duplicate sample = 10.02 ng/mL; re-analysis three days later = 10.8 ng/mL (during re-analysis a Cr(III) peak was also identified and quantified at 0.536 ng/mL, but this was due to a baseline interference)

Results notes

-Based on speciation analysis of water samples, the intended exposure species for each tank was detected as expected. Furthermore, the speciation results and chromatographs suggest that there was no conversion between Cr(III) and Cr(VI) in water samples. More specifically, no Cr(VI) was detected in tank water spiked with Cr(III) only and no Cr(III) was detected in tank water spiked with Cr(VI) only. However, to confirm this quantitatively, a method that allows for the tracing of conversion, such as Speciated Isotope Dilution Mass Spectrometry (SIDMS; EPA 6800), would be required.
-However, our results suggest that the amount of Cr was lower in all treatments than expected, by approximately 50%. Long-term storage of acidified samples may have dampened the detection some elements through ICP-MS. But, given the agreement among all analytical runs for both total Cr and IC speciation analysis within samples, this seems unlikely have had a significant impact.

Suggested supplement information (SI)

Table SI-1: Total chromium (Cr) results from the three test dates in 2021. Results presented were analyzed in DRC gas mode. *Speciation samples checked for total values were diluted 10X before analysis to reduce solute loading on the ICP-MS.

Sample ID	Tank/sample Info	Feb 11th/12th	April 12th	April 13th
Samples				
CT-1*	Cr3+, 20µg/L	12.65	11.37	---
CT-2	Cr3+, 20µg/L DUP	---	---	---
CT-3	Cr3+, 0.2µg/L	---	---	---
CT-4	Cr3+, 0.2µg/L DUP	---	---	---
CT-5*	CrPic, 20µg/L	3.21	2.62	---
CT-6	CrPic, 20µg/L DUP	---	---	---
CT-7*	Cr6+, 20 µg/L	10.34	8.53	---
CT-8	Cr6+, 20 µg/L DUP	---	---	---
CT-9	Cr6+, 0.2µg/L	---	---	---
CT-10	Cr6+, 0.2µg/L DUP	---	---	---
CT-11	T.Cr3+, 20µg/L - Total Cr	11.374	11.367	10.399
CT-12	T.Cr3+, 0.2µg/L - Total Cr	0.237	0.244	---
CT-13	T.Cr6+, 20µg/L - Total Cr	8.563	7.831	---
CT-14	T.Cr6+, 0.2µg/L - Total Cr	0.191	0.252	---
CT-15	T.CrPic, 20µg/L - Total Cr	1.456	1.357	---
CT-16	DI - DI Control	0.092	0.098	---
CT-17	MilliQ - MilliQ Control	0.090	0.090	0.045
CT-18	Cr3+, 100µg/L - 20 µg/L 5x Spike	2.298	---	---
CT-19	Cr3+, 1µg/L - 0.2 µg/L 5x Spike	0.131	---	---
CT-20	Cr6+, 100µg/L - 20 µg/L 5x Spike	3.124	---	---
CT-21	Cr6+, 1µg/L - 0.2 µg/L 5x Spike	0.162	---	---
CT-22	CrPic, 100µg/L - 20 µg/L 5x Spike	1.072	---	---
Quality Assurance and Control (QAQC)[4]				
QAQC-1	Water CRM (20µg/L), % Recovery	116.2%	106.6%	99.7%, 100.4% (n = 2)
QAQC-2	Instrument spike (5µg/L), % Recovery	97.4%	35.1%	98.6%
QAQC-3	Instrument spike (1µg/L), % Recovery	82.3%	---	---
QAQC-4	Duplicate, % Difference	---	-10.8 to 13.4% (n = 4)	0.5%[3]
QAQC-5	Calibration standards, % Deviation from expected	-15.7 to 5.4%	-0.36 to 0.28%	-0.17 to 0.45%
QAQC-6	Internal Standard, % Recovery range in samples	34.2 to 44.0%[1]	79.3 to 96.9%[2]	94.1 to 104.0%
QAQC-7	Internal Standard, % Recovery range in standards	49.2 to 51.6%	97.0 to 101.4%	97.3 to 100.9%
QAQC-8	Range in RSDs of concentrations	0.1 to 13.5%[5]	0.7 to 8.2%	1.3 to 2.7%

[1]Recoveries are low, but match the standards in the calibration curve, which likely accounted for the issue. [2]Note, only samples preserved for speciation had IS recoveries < 80%; this is likely due to the high solute concentrations dampening the signal; [3]When compared to the April 12th result; [4]N = 1 unless otherwise stated; [5]One speciation sample had a high RSD (13.5%), while all other sample RSDs were < 7.5%. (**Calculations**: % Deviation = ((result – expected) / expected) *100; % Recovery = (results/expected)*100; % Difference = ((original – duplicate) / ((original + duplicate)/2)) *100).

Stability trials of Cr(III) and Cr(VI) speciation after preservation with 50mM NaOH, 28mMNa2CO3, and 10mM EDTA

In the first stability, three samples were prepared in 25mL at a concentration of 20 ng/mL of Cr(III) and 20 ng/mL Cr(VI); a fourth sample was left un-spiked as a method blank. Approximately 0.05g of NaOH, 0.075g of Na_2CO_3, and 0.05g of EDTA were added to all samples to achieve desired molarities for preservation of Cr species. One of the three spiked samples and the method blank were inverted 10 times but were not heated in any way. The remaining two spiked samples were heated through sonication (at 60˚C for 60 mins) or a hot block (at 95˚C for 60 mins). After cooling to room temperature, all samples were stored at approximately 4˚C for 5 days before analysis by IC-ICP-MS, the results from which are shown in Table SI-2.

Table SI-2. The percent recoveries of 20 ng/mL speciated chromium spikes during stability testing of the water preservation method using three heating methods. Only one analysis was conducted, 5-days after spiking. NA = not analyzed. One method blank was also analyzed; no Cr(III) or Cr(VI) were detected.

Heating Method	Cr Species	Conc. (ng/mL)	% Recovery
Method Blank	Cr(III)	0.146	---
	Cr(VI)	0.083	---
No Heat	Cr(III)	1.729	86.5
	Cr(VI)	2.072	103.6
Sonicator (60˚C for 60 mins)	Cr(III)	1.847	92.4
	Cr(VI)	2.098	104.9
Hot Block (95˚C for 60 mins)	Cr(III)	2.038	101.9
	Cr(VI)	2.275	113.8

In the second stability trial, samples were spiked with both Cr(III) and Cr(VI) generally following the same procedure as described above. In this trial, two concentrations were tested: a low-level (3 ng/mL, n = 6) and a high-level (30 ng/mL, n = 6). Additionally, method blanks (i.e., with no Cr spikes, n = 6) and single-species samples (i.e., only Cr(III) or only Cr(VI) spikes) at 30 ng/mL (n = 2) were made. Half of these samples (i.e., 3 low-level, 3 high-level, 3 blanks, 2 single-species) were inverted 10-times after spiking and not heated, while the other half (i.e., 3 low-level, 3 high-level, 3 blanks, 2 single-species) were inverted 10-times and heated on a hot-plate to 60˚C for 60-mins. All samples were stored at 4˚C after creation and in-between analytical time-points. All samples were analyzed approximately (1) 3-5 hours, (2) 24-hours, and (3) 7-days after creation. In general, the results showed high recovery of Cr(III) and Cr(VI) method spikes at 30 ng/mL across all time points (94.1 to 111.6% recovery; Table SI-3 and Figure SI-1). However, the low-level spike of 3 ng/mL showed high recoveries approximately 5-hours after spiking for both Cr species (88.7 to 112.0%), but these recoveries declined 48-hours (67.7 to 125.7%) and 7-days (41.8 to 130.7%) after spiking (Table SI-2). These findings suggest some interconversion during storage. However, samples with single-species spiked showed no evidence of conversion through the lack of detection of the opposing species (Table SI-3). It is also noteworthy that the Cr(III) chromatography peak deteriorated over time. This observation was more pronounced in the low-level spiked samples (i.e., 3 ng/mL; Figure SI-1a-c), but was also seen to a lesser extent in the 7-day time point in the samples spiked at the higher-level (i.e., 30 ng/mL; Figure SI-1f).

Table SI-3. The percent recoveries of speciated chromium spikes during stability testing of the water preservation method. NA = not analyzed. Six blanks, three heated and three unheated, were also analyzed at all time points; no Cr(III) or Cr(VI) was detected at any point.

Sample Label	Sample Description	Initial		24-hour		7-day	
		Cr(III)	Cr(VI)	Cr(III)	Cr(VI)	Cr(III)	Cr(VI)
Non-heated samples							
R4-4	3 ng/mL Cr(III) + 3 ng/mL Cr(VI)[1]	89.2	101.8	67.7	119.3	45.2[2]	128.0
R4-5	3 ng/mL Cr(III) + 3 ng/mL Cr(VI) [1]	88.7	98.8	74.0	121.2	41.8[2]	119.0
R4-6	3 ng/mL Cr(III) + 3 ng/mL Cr(VI) [1]	95.0	105.5	83.3	121.7	55.7[2]	126.2
R4-7	30 ng/mL Cr(III) + 30 ng/mL Cr(VI)	105.1	99.3	101.2	102.4	105.6[2]	106.3
R4-8	30 ng/mL Cr(III) + 30 ng/mL Cr(VI)	101.4	99.1	100.8	101.8	114.8[2]	105.4
R4-9	30 ng/mL Cr(III) + 30 ng/mL Cr(VI)	102.4	102.0	99.6	101.3	104.8[2]	105.3
R4-10	30 ng/mL Cr(III)	98.5	---	94.1	---	101.4[2]	---
R4-11	30 ng/mL Cr(VI)	---	97.0	---	100.2	---	103.1
Heated samples, 80˚C for 60 mins							
R4-15	3 ng/mL Cr(III) + 3 ng/mL Cr(VI) [1]	104.7	106.7	83.3	115.0	101.3[2]	128.2
R4-16	3 ng/mL Cr(III) + 3 ng/mL Cr(VI) [1]	96.2	108.0	72.0	125.7	101.5[2]	130.0
R4-17	3 ng/mL Cr(III) + 3 ng/mL Cr(VI) [1]	98.2	112.0	75.8	118.5	104.0[2]	130.7
R4-18	30 ng/mL Cr(III) + 30 ng/mL Cr(VI)	NA	NA	100.3	104.1	109.1[2]	107.5
R4-19	30 ng/mL Cr(III) + 30 ng/mL Cr(VI)	111.6	103.8	102.7	101.7	109.6[2]	109.5
R4-20	30 ng/mL Cr(III) + 30 ng/mL Cr(VI)	111.5	102.3	104.2	104.5	106.8[2]	111.2
R4-21	30 ng/mL Cr(III)	107.8	---	98.4	---	103.5[2]	---
R4-22	30 ng/mL Cr(VI)	---	99.9	---	105.2	---	101.7

[1]Samplesd were diluted 5X before analysis; 10X dilutions were also checked periodically for accuracy; [2]Chromatographic peak was split and had to be manually integrated.

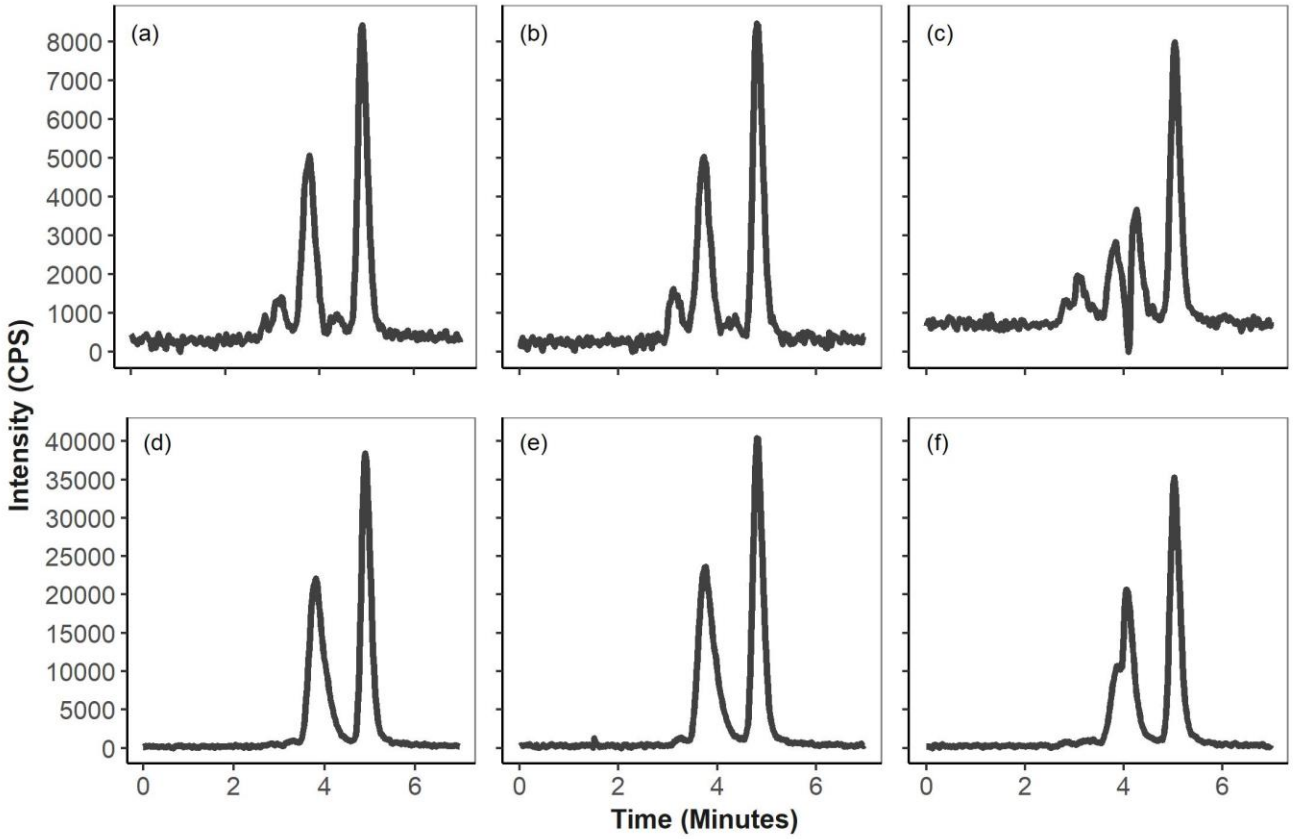

Figure SI-1. Chromatographs of low-level (a-c) and high-level (d-f) spikes of Cr(III) and Cr(VI) over 3 time periods: initial readings (a, d), 24-hours after creation (b, e), and 7-days after creation (c, f).

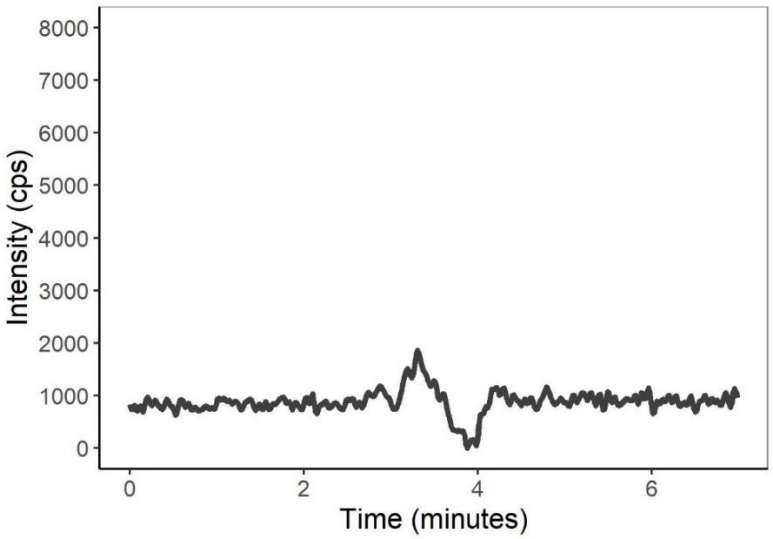

Figure SI-2. Chromatograph of the baseline disturbance present around the retention time of Cr(III).

BIBLIOGRAPHY

1. Beukes JP, du Preez SP, van Zyl PG, Paktunc D, Fabritius T, Päätalo M, et al. Review of Cr(VI) environmental practices in the chromite mining and smelting industry – Relevance to development of the Ring of Fire, Canada. Journal of Cleaner Production. 2017;165:874-89.
2. Kotaś J, Stasicka Z. Chromium occurrence in the environment and methods of its speciation. Environmental Pollution. 2000;107(3):263-83.
3. Anderson RA, Bryden NA, Polansky MM. Lack of toxicity of chromium chloride and chromium picolinate in rats. Journal of the American College of Nutrition. 1997;16(3):273-9.
4. B. D. Kerger B. L. Finley G. E. Corbett DGDDJP. Ingestion of chromium(VI) in drinking water by human volunteers: Absorption, disruption, and excretion of single and repeated doses. Journal of Toxicology and Environmental Health. 1997;50(1):67-95.
5. Standeven AM, Wetterhahn KE. Chromium(VI) Toxicity: Uptake, Reduction, and DNA Damage. Journal of the American College of Toxicology. 1989;8(7):1275-83.
6. DeFlora S, Camoirano A, Bagnasco M, Bennicelli C, Corbett GE, Kerger BD. Estimates of the chromium(VI) reducing capacity in human body compartments as a mechanism for attenuating its potential toxicity and carcinogenicity. Carcinogenesis. 1997;18(3):531-7.
7. Norseth T. The carcinogenicity of chromium. Environ Health Perspect. 1981;40:121-30.
8. Costa M. Potential hazards of hexavalent chromate in our drinking water. Toxicology and Applied Pharmacology. 2003;188(1):1-5.
9. Costa M, Klein CB. Toxicity and Carcinogenicity of Chromium Compounds in Humans. Critical Reviews in Toxicology. 2006;36(2):155-63.
10. Eastmond DA, MacGregor JT, Slesinski RS. Trivalent chromium: Assessing the genotoxic risk of an essential trace element and widely used human and animal nutritional supplement. Critical Reviews in Toxicology. 2008;38(3):173-90.
11. Anderson RA. Chromium as an Essential Nutrient for Humans. Regulatory Toxicology and Pharmacology. 1997;26(1):S35-S41.
12. Kerger BD, Paustenbach DJ, Corbett GE, Finley BL. Absorption and elimination of trivalent and hexavalent chromium in humans following ingestion of a bolus dose in drinking water. Toxicology and Applied Pharmacology. 1996;141(1):145-58.
13. Lescord GL, Johnston TA, Heerschap MJ, Keller W, Southee FM, O'Connor CM, et al. Arsenic, chromium, and other elements of concern in fish from remote boreal lakes and rivers: Drivers of variation and implications for subsistence consumption. Environmental Pollution. 2020;259:113878.
14. Stearns DM, Kennedy LJ, Courtney KD, Giangrande PH, Phieffer LS, Wetterhahn KE. Reduction of Chromium(VI) by Ascorbate Leads to Chromium-DNA Binding and DNA Strand Breaks in Vitro. Biochemistry. 1995;34(3):910-9.
15. Levina A, Lay PA. Chemical Properties and Toxicity of Chromium(III) Nutritional Supplements. Chemical Research in Toxicology. 2008;21(3):563-71.
16. Bona K, Love S, Rhodes N, McAdory D, Sinha S, Kern N, et al. Chromium is not an essential trace element for mammals: effects of a 'low-chromium' diet. Journal of Biological Inorganic Chemistry. 2011;16(3):381-90.

17. Shi X. Reduction of chromium(VI) and its relationship to carcinogenisis. Journal of Toxicology and Environmental Health, Part B. 1999;2(1):87-104.
18. Tsapakos MJ, Hampton TH, Wetterhahn KE. Chromium(VI)-induced DNA Lesions and Chromium Distribution in Rat Kidney, Liver, and Lung. Cancer Research. 1983;43(12 Part 1):5662.
19. Brauer SL, Wetterhahn KE. Chromium(VI) forms a thiolate complex with glutathione. Journal of the American Chemical Society. 1991;113(8):3001-7.
20. Chan HM, Fediuk K, Batal M, Sadik T, Tikhonov C, Ing A, et al. The First Nations Food, Nutrition and Environment Study (2008–2018)—rationale, design, methods and lessons learned. Canadian Journal of Public Health. 2021;112(1):8-19.
21. Yilmaz AB, Turan C, Toker T. Uptake and distribution of hexavalent Cr in tissues (gill, skin and muscle) of a freshwater fish, Tilapia, Oreochromis aureus. JECE. 2010;2:28-33.
22. Chen H, Cao J, Li L, Wu X, Bi R, Klerks PL, et al. Maternal transfer and reproductive effects of Cr(VI) in Japanese medaka (Oryzias latipes) under acute and chronic exposures. Aquatic Toxicology. 2016;171:59-68.
23. Van Der Putte I, Lubbers J, Kolar Z. Effect of pH on uptake, tissue distribution and retention of hexavalent chromium in rainbow trout (Salmo gairdneri). Aquatic Toxicology. 1981;1(1):3-18.
24. Chen H, Mu L, Cao J, Mu J, Klerks PL, Luo Y, et al. Accumulation and effects of Cr(VI) in Japanese medaka (Oryzias latipes) during chronic dissolved and dietary exposures. Aquatic Toxicology. 2016;176:208-16.
25. Roberts AP, Oris JT. Multiple biomarker response in rainbow trout during exposure to hexavalent chromium. Comparative Biochemistry and Physiology Part C: Toxicology & Pharmacology. 2004;138(2):221-8.
26. Al-Akel AS, Shamsi MJK. Hexavalent chromium: Toxicity and impact on carbohydrate metabolism and haematological parameters of carp (Cyprinus carpio L.) from Saudi Arabia. Aquatic Sciences. 1996;58(1):24-30.
27. Vutukuru SS. Chromium Induced Alterations in Some Biochemical Profiles of the Indian Major Carp, Labeo rohita (Hamilton). Bulletin of Environmental Contamination and Toxicology. 2003;70(1):0118-23.
28. Stearns DM, Wetterhahn KE. Intermediates Produced in the Reaction of Chromium(VI) with Dehydroascorbate Cause Single-Strand Breaks in Plasmid DNA. Chemical Research in Toxicology. 1997;10(3):271-8.
29. Lay PA, Levina A. Kinetics and Mechanism of Chromium(VI) Reduction to Chromium(III) by l-Cysteine in Neutral Aqueous Solutions. Inorganic Chemistry. 1996;35(26):7709-17.
30. Abdullah M, Barrett J, O'Brien P. Synthesis and characterization of some chromium(III) complexes with glutathione. Journal of the Chemical Society, Dalton Transactions. 1985(10):2085-9.
31. Codd R, Dillon CT, Levina A, Lay PA. Studies on the genotoxicity of chromium: from the test tube to the cell. Coord Chem Rev. 2001;216:537-82.
32. Westheimer FH. The Mechanisms of Chromic Acid Oxidations. Chemical Reviews. 1949;45(3):419-51.

33. Wiberg KB, Szeimies G. Oxidation of aldehydes by chromium(VI) and by chromium(V) in 96% acetic acid. Journal of the American Chemical Society. 1974;96(6):1889-92.
34. Krepkiy D, Antholine WE, Myers C, Petering DH. Model reactions of Cr (VI) with DNA mediated by thiol species. Molecular and Cellular Biochemistry. 2001;222(1):213-9.
35. Connett PH, Wetterhahn KE. In vitro reaction of the carcinogen chromate with cellular thiols and carboxylic acids. Journal of the American Chemical Society. 1985;107(14):4282-8.
36. Kwong DWJ, Pennington DE. Stoichiometry, kinetics, and mechanisms of the chromium(VI) oxidation of L-cysteine at neutral pH. Inorganic Chemistry. 1984;23(16):2528-32.
37. Stearns DM, Wetterhahn KE. Reaction of Chromium(VI) with Ascorbate Produces Chromium(V), Chromium(IV), and Carbon-Based Radicals. Chemical Research in Toxicology. 1994;7(2):219-30.
38. Tsou T-C, Yang J-L. Formation of reactive oxygen species and DNA strand breakage during interaction of chromium(III) and hydrogen peroxide in vitro: evidence for a chromium(III)-mediated Fenton-like reaction. Chemico-Biological Interactions. 1996;102(3):133-53.
39. Sugden KD, Wetterhahn KE. Identification of the Oxidized Products Formed upon Reaction of Chromium(V) with Thymidine Nucleotides. Journal of the American Chemical Society. 1996;118(44):10811-8.
40. Liu KJ, Jiang JJ, Swartz HM, Shi XG. Low-Frequency EPR Detection of Chromium(V) Formation by Chromium(VI) Reduction in Whole Live Mice. Archives of Biochemistry and Biophysics. 1994;313(2):248-52.
41. Levina A, Barr-David G, Codd R, Lay PA, Dixon NE, Hammershøi A, et al. In Vitro Plasmid DNA Cleavage by Chromium(V) and -(IV) 2-Hydroxycarboxylato Complexes. Chemical Research in Toxicology. 1999;12(4):371-81.
42. Wang Y-q, Yao M-h. Effects of chromium picolinate on glucose uptake in insulin-resistant 3T3-L1 adipocytes involve activation of p38 MAPK. The Journal of Nutritional Biochemistry. 2009;20(12):982-91.
43. Saltiel AR, Kahn CR. Insulin signalling and the regulation of glucose and lipid metabolism. Nature. 2001;414(6865):799-806.
44. Hua Y, Clark S, Ren J, Sreejayan N. Molecular mechanisms of chromium in alleviating insulin resistance. The Journal of Nutritional Biochemistry. 2012;23(4):313-9.
45. Myers MG, Jr., White MF. The new elements of insulin signaling: insulin receptor substrate-1 and proteins with SH2 domains. Diabetes. 1993 1993/05//:643+.
46. Vincent JB. Quest for the Molecular Mechanism of Chromium Action and Its Relationship to Diabetes. Nutrition Reviews. 2000;58(3):67-72.
47. Vincent JB. Elucidating a Biological Role for Chromium at a Molecular Level. Accounts of Chemical Research. 2000;33(7):503-10.
48. Shen Y, Kim J, Strittmatter EF, Jacobs JM, Camp Ii DG, Fang R, et al. Characterization of the human blood plasma proteome. Proteomics. 2005;5(15):4034-45.
49. Eames SC, Philipson LH, Prince VE, Kinkel MD. Blood sugar measurement in zebrafish reveals dynamics of glucose homeostasis. Zebrafish. 2010;7:205+.

50. Hussain B, Sultana T, Sultana S, Masoud MS, Ahmed Z, Mahboob S. Fish eco-genotoxicology: Comet and micronucleus assay in fish erythrocytes as in situ biomarker of freshwater pollution. Saudi Journal of Biological Sciences. 2018;25(2):393-8.
51. Wannee Jiraungkoorskul PK, Somphong Sahaphong, Pukaew Kirtputra, Jasmin Chawlab and Shanida Charucharoen. Evaluation of Micronucleus Test's Sensitivity in Freshwater Fish Species. Research Journal of Environmental Sciences. 2011;1(2):56 - 63.
52. Alkaladi A, Nasr El- Deen N, Afifi M, Zinadah O. Hematological and biochemical investigations on the effect of vitamin E and C on Oreochromis niloticus exposed to zinc oxide nanoparticles. Saudi Journal of Biological Sciences. 2015;608.
53. Atanas Kamburov CW, Hans Lehrach, Ralf Herwig. ConsensusPathDB--a database for integrating human functional interaction networks. Nucleic Acids Research. 2009;37:D623-D8.
54. Atanas Kamburov KP, Hanna Galicka, Christoph Wierling, Hans Lehrach, Ralf Herwig. ConsensusPathDB: toward a more complete picture of cell biology. Nucleic Acids Research. 2011;39:D712-7.
55. Hatakeyama S. TRIM Family Proteins: Roles in Autophagy, Immunity, and Carcinogenesis. Trends in Biochemical Sciences. 2017;42(4):297-311.
56. Ding Q, He D, He K, Zhang Q, Tang M, Dai J, et al. Downregulation of TRIM21 contributes to hepatocellular carcinoma carcinogenesis and indicates poor prognosis of cancers. Tumor Biology. 2015;36(11):8761-72.
57. Liao DK, Seto M, Noma K. Rho kinase (ROCK) inhibitors. Journal Of Cardiovascular Pharmacology. 2007;50(1):17-24.
58. Koch J, Tönges L, Barski E, Michel U, Bähr M, Lingor P. ROCK2 is a major regulator of axonal degeneration, neuronal death and axonal regeneration in the CNS. Cell Death & Disease. 2014.
59. Field SD, Arkin J, Li J, Jones LH. Selective Downregulation of JAK2 and JAK3 by an ATP-Competitive pan-JAK Inhibitor. ACS Chemical Biology. 2017;12(5):1183-7.
60. Khananshvili D. The SLC8 gene family of sodium–calcium exchangers (NCX) – Structure, function, and regulation in health and disease. Molecular Aspects of Medicine. 2013;34(2):220-35.
61. Ottolia M, Nicoll DA, Philipson KD. Roles of Two Ca2+-binding Domains in Regulation of the Cardiac Na+-Ca2+ Exchanger*. Journal of Biological Chemistry. 2009;284(47):32735-41.
62. Mezquita J, Mezquita B, Pau M, Mezquita C. Down-regulation of Flt-1 gene expression by the proteasome inhibitor MG262. Journal of Cellular Biochemistry. 2003;89(6):1138-47.
63. von Kleeck R, Castagnino P, Roberts E, Talwar S, Ferrari G, Assoian RK. Decreased vascular smooth muscle contractility in Hutchinson–Gilford Progeria Syndrome linked to defective smooth muscle myosin heavy chain expression. Scientific Reports. 2021;11(1):10625.
64. Carniel E, Taylor MRG, Sinagra G, Di Lenarda A, Ku L, Fain PR, et al. α-Myosin Heavy Chain. Circulation. 2005;112(1):54-9.
65. Charvet B, Guiraud A, Malbouyres M, Zwolanek D, Guillon E, Bretaud S, et al. Knockdown of col22a1 gene in zebrafish induces a muscular dystrophy by disruption of the myotendinous junction. Development. 2013;140(22):4602-13.

66. Shaw P, Mondal P, Bandyopadhyay A, Chattopadhyay A. Environmentally relevant concentration of chromium activates Nrf2 and alters transcription of related XME genes in liver of zebrafish. Chemosphere. 2019;214:35-46.
67. Farag AM, May T, Marty GD, Easton M, Harper DD, Little EE, et al. The effect of chronic chromium exposure on the health of Chinook salmon (Oncorhynchus tshawytscha). Aquatic Toxicology. 2006;76(3):246-57.
68. Bakshi A, Panigrahi AK. A comprehensive review on chromium induced alterations in fresh water fishes. Toxicol Rep. 2018;5:440-7.
69. de Lemos CT, Rödel PM, Terra NR, Erdtmann B. Evaluation of basal micronucleus frequency and hexavalent chromium effects in fish erythrocytes. Environmental Toxicology and Chemistry. 2001;20(6):1320-4.
70. Hatakeyama S. TRIM proteins and cancer. Nature Reviews Cancer. 2011;11(11):792-804.
71. Costa M. Toxicity and Carcinogenicity of Cr(VI) in Animal Models and Humans. Critical Reviews in Toxicology. 1997;27(5):431-42.
72. Uhlén M ea. Tissue-based map of the human proteome. Science. 2015.
73. Heijman J, Schirmer I, Dobrev D. The multiple proarrhythmic roles of cardiac calcium-handling abnormalities: triggered activity, conduction abnormalities, beat-to-beat variability, and adverse remodelling. EP Europace. 2016;18(10):1452-4.
74. Schiaffino S, Rossi AC, Smerdu V, Leinwand LA, Reggiani C. Developmental myosins: expression patterns and functional significance. Skeletal Muscle. 2015;5(1):22.
75. Kiehart DP. Molecular genetic dissection of myosin heavy chain function. Cell. 1990;60(3):347-50.
76. Yang D, Han B, Baiyun R, Lv Z, Wang X, Li S, et al. Sulforaphane attenuates hexavalent chromium-induced cardiotoxicity via the activation of the Sesn2/AMPK/Nrf2 signaling pathway. Metallomics. 2020;12(12):2009-20.
77. Yang D, Yang Q, Fu N, Li S, Han B, Liu Y, et al. Hexavalent chromium induced heart dysfunction via Sesn2-mediated impairment of mitochondrial function and energy supply. Chemosphere. 2021;264:128547.
78. Castro MP, de Moraes FR, Fujimoto RY, da Cruz C, de Andrade Belo MA, de Moraes JRE. Acute Toxicity by Water Containing Hexavalent or Trivalent Chromium in Native Brazilian Fish, Piaractus mesopotamicus: Anatomopathological Alterations and Mortality. Bulletin of Environmental Contamination and Toxicology. 2014;92(2):213-9.
79. Nagpure NS, Srivastava R, Kumar R, Kushwaha B, Srivastava SK, Kumar P, et al. Assessment of genotoxic and mutagenic potential of hexavalent chromium in the freshwater fish Labeo rohita (Hamilton, 1822). Drug & Chemical Toxicology. 2015;38(1):9-15.
80. Ussery E, Bridges KN, Pandelides Z, Kirkwood AE, Guchardi J, Holdway D. Developmental and Full-Life Cycle Exposures to Guanylurea and Guanylurea–Metformin Mixtures Results in Adverse Effects on Japanese Medaka (Oryzias latipes). Environmental Toxicology and Chemistry. 2019;38(5):1023-8.